REVISTA VIRTUAL DEL
INSTITUTO DE FISICA "LUIS RIVERA TERRAZAS"
UNIVERSIDAD AUTONOMA DE PUEBLA

Editores: F. Pérez Rodríguez y F. Rivas Silva

No.2, 2000

Quantum Chaos and Thermalization for Interacting Particles

(NOTAS DE CURSO)

F.M. Izrailev
Instituto de Física, Universidad Autónoma de Puebla,
Apdo. Post. J-48, Puebla, Pue. 72570, México

Prólogo

Estas son unas notas del curso impartido en The International School of Physics "Enrico Fermi" (Varenna, ITALIA, Julio de 1999). El material de estas notas también ha sido utilizado en el curso optativo "Temas selectos de la física teórica (caos, cuantización y teoría de muchos cuerpos)" del Doctorado en Ciencias (Física) del Instituto de Física de la BUAP. Pueden ser útiles para estudiantes interesados en la teoría del Caos Cuántico y sus aplicaciones a la física atómica, nuclear, de estado sólido, de puntos cuánticos, etc.

En estas notas se presenta una revisión sobre el problema actual de partículas interactuantes en sistemas cuánticos aislados. Como es sabido, en la mecánica clásica la interacción entre partículas comúnmente conduce al inicio del caos el cual permite describir sistemas dinámicos de una manera estadística. El punto importante es que el movimiento de un sistema clásico puede tener propiedades caóticas aún para un número muy pequeño (dos o más) de partículas (interactuantes). El mecanismo de este fenómeno es una inestabilidad extremadamente fuerte del movimiento debida al carácter no lineal de la equación de movimiento de Newton.

Contrariamente a la mecánica clásica, en un sistema cuántico aislado no hay inestabilidad del movimiento ya que el espectro de energía es discreto y el movimiento de un sistema siempre es cuasi-periódico. Sin embargo, un tipo de complejidad del movimiento ocurre también en los sistemas cuánticos los cuales son caóticos en el límite clásico. Esta situación se conoce como el "caos cuántico". En tal situación, la aproximación estadística parece ser también válida para sistemas aislados.

En estas notas de curso, el problema de la descripción de sistemas cuánticos aislados se trata en detalle. Se sugiere un nuevo método que se basa en una estructura caótica de auto-valores. Este método es válido tanto para sistemas desordenados sin límite clásico como para sistemas dinámicos que son caóticos en el límite clásico.

Para mostrar este enfoque, se considera un modelo específico que ahora es conocido como el "modelo de interacción aleatoria de dos cuerpos". En este modelo se supone que la interacción de dos cuerpos es completamente caótica, por lo que surge la pregunta: ¿Cuáles son las propiedades del sistema en este límite "caótico" extremo? Resulta que a pesar de la completa aleatoriedad de la interacción, el sistema puede ser descrito estadísticamente bajo condiciones específicas. En las presentes notas de curso discutimos esas condiciones y mostramos como un enfoque estadístico puede ser desarrollado cuando las condiciones son satisfechas. Se ha puesto una atención particular al arranque de la termalización y la posibilidad de introducir una temperatura del sistema aislado con propiedades caóticas.

Existen muchas situaciones físicas donde el enfoque sugerido puede aplicarse: átomos complejos, moléculas y núcleos, cúmulos atómicos, espines interactuantes, etc.

F.M. Izrailev

Prólogo traducido del idioma inglés al español por F. Pérez Rodríguez

Quantum Chaos and Thermalization for Interacting Particles

F.M.Izrailev
Instituto de Física, Universidad Autonoma de Puebla, Apdo. Postal J-48, Puebla, 72570 México

In this review the problem of statistical description of isolated quantum systems of interacting particles is discussed. Main attention is paid to a recently developed approach which is based on chaotic properties of compound states in the basis of non-interacting particles. In order to demonstrate the most important aspects of this approach, the matrix model of two-body random interaction between Fermi-particles has been used. Different problems have been considered such as the onset of chaos and statistical equilibrium, the relation between the structure of eigenstates and distribution of occupation numbers, the emergence of the Fermi-Dirac distribution in isolated systems of finite number of particles and many others. The application of the approach to dynamical systems with the classical limit is discussed as well.

PACS numbers: 05.45.+b, 31.25.-v, 31.50.+w, 32.30.-r

I. INTRODUCTION

Until recently, the *quantum chaos theory* was mainly related to few-body physics. On the other hand, in real physical systems such as many-electron atoms and heavy nuclei, the origin of complex behavior is quite strong interaction between many particles. To deal with such systems, famous statistical approach has been developed which is based on the *Random Matrix Theory* (RMT) (see, for example, [1–4]). The main idea of this approach is to forget about a detailed description of the motion and to treat these systems statistically having in mind that the interaction between particles is so complex and strong that generic properties are expected to emerge. Simplest models of the RMT are full random matrices of a given symmetry, the latter was shown to have a direct link with underlying symmetries of physical systems.

One of the main results of the RMT is the prediction of a specific kind of correlations in the energy spectra of complex quantum systems. Among many characteristics of these correlations, the most popular is the distribution of spacings between nearest energy levels in the spectra. Exact analytical expression of this distribution is very complicated, instead, one uses the so-called Wigner-Dyson (WD) surmise (quite simple expression which gives a very good approximation to the exact result). A distinctive property of this *WD-distribution* is the repulsion between neighboring levels in the spectra, the degree of this repulsion (linear, quadratic or quartic) depends on the symmetry of random matrices. In fact, such type of repulsion was observed experimentally very long ago (first experimental observation is reported in Ref. [5] for the energy spectra of heavy nuclei), and discussed in many theoretical works.

After this prediction of the RMT, the WD-distribution has been confirmed to occur in heavy nuclei and many-electron atoms, see references in [3,6]. Later on, it was found also in dynamical systems with chaotic behavior in the classical limit, famous examples are the so-called billiards (see for example, [6]). As a result, it was understood that chaotic properties of quantum systems are generic for both disordered models (when the randomness of matrix elements is postulated from the beginning) and dynamical systems for which the pseudo-randomness appears as a result of special conditions, the latter are convenient to explain by comparing with the classical limit. Thus, one can say that limiting properties of quantum chaos in the case when all regular dynamical effects are neglected, are described by the RMT.

As one can see, the RMT can give a proper description of a system (mainly, the properties of energy spectra) only locally, in a restricted region of energy spectra. Indeed, the RMT can not give any global energy dependence neither for the energy spectrum nor for eigenstates, it is parameter-independent theory. In this sense, the conventional RMT (ensembles of fully random matrices) is very restricted and, for example, it can not be directly applied to such important phenomena as the localization of eigenstates in disordered models. This is why new approaches in the RMT have been developed by imposing internal structure of random matrices. The most known example is the so-called *Band Random Matrices* (BRM), or random matrices with a band-like structure (see, for example, [7], [8] and references therein). Inside the band, the matrix elements are assumed to be random and independent, and outside the band matrix elements are set to zero. The BRM-ensemble has been recently studied in details both numerically and theoretically, and much is now known about the structure of eigenstates and spectrum statistics for both infinite and finite matrices. The application of this kind of matrices in physics is very broad. In particular, they have been used to describe dynamical localization in dynamical systems with time-periodic perturbation (paradigmatic model is the Kicked Rotor [7]), and the localization of eigenstates in quasi-1d disordered models in solid state physics [8].

Another class of band random matrices has been introduced very long ago by Wigner in Ref. [9]. The structure of these *Wigner Band Random Matrices* (WBRM) is characterized by the *leading diagonal* with reordered (in an increasing way) values, plus random and independent off-diagonal elements inside the band of size b. This type of matrices is much closer to physical realistic systems, compared to the standard full random matrices. One can suggest that the original motivation of Wigner for the study of these matrices was a close correspondence to Hamiltonians of complex nuclei, which are typically described by the mean-field part H_0 (leading diagonal) and the residual interaction V of the finite energy range (off-diagonal matrix elements inside the band). The main interest of Wigner was the quantity which nowadays is known as the *strength function* or *local density of states* (LDOS). This quantity is extremely important when describing the spread of energy, initially concentrated in a specific state of the unperturbed Hamiltonian H_0, between all other states due to the internal interaction V . In particular, it was analytically shown that this function has the form of the Lorentzian if interaction is sufficiently (but not extremely) large. This result is fundamental and it is used in very different applications.

However, in spite of the success of the standard RMT and its modern developments, the strong assumption of randomness of matrix elements, as well as a specific (band) structure of matrices do not allow to relate such matrices directly to realistic many-particle Hamiltonians. One of the important reasons is that the underlying structure of realistic Hamiltonian matrices results from the single-particle spectrum and *two-body interaction* between particles. In order to understand the role of $k-$body (random) interaction, a new ensemble of matrices has been suggested (see, for example, [10,11,3] and references therein). In this approach the matrices arise as a result of construction from the single-particle basis, provided random character of the $k-$body interaction. The study of this ensemble of matrices have shown that even when the interaction V is very strong and the influence of the leading diagonal may be neglected, there are serious differences from the standard RMT. In particular, it was discovered that for the two-body interaction, $k = 2$, the spectral fluctuations are different from those predicted by the RMT, although the distribution of spacing between nearest levels has the form similar to the WD-distribution. It was shown that full random matrices occur when the rank of interaction is very large, $k \to \infty$.

Due to very serious mathematical problems these *two-body random interaction* (TBRI) matrices were forgotten for quite a long time, and only recently they have been used in the context of quantum chaos. In these lectures, the author gives a review of recent results obtained for the TBRI-model in collaboration with the co-authors. Main attention is paid to a novel approach developed in [12–16], which is based on the chaotic structure of eigenstates in a given basis of unperturbed many-particle states. This approach allows to relate statistical properties of exact eigenstates in many-body representation directly to properties of single-particle operators, in the first line, to the occupation number distribution of single-particle states.

The structure of the paper is as follows. In the next Section 2.1 the structure of the TBRI-matrices is discussed in details. It was explained how these matrices are constructed from single-particle states and what are properties of matrix elements in many-body representation, also, the comparison is made with full random matrices. A particular point is that in spite of complete randomness and independence of two-body matrix elements, off-diagonal matrix elements of many-particle Hamiltonian matrices have underlying correlations which are due to a two-body nature of interaction.

In Section 2.2 generic properties of density of states and level spacing distribution are briefly discussed, although they are not the main interest of the study. Section 2.3 deals with the structure of exact eigenstates in dependence on the interaction strength and excitation energy. The notion of the average shape of the eigenstates ($F-$*function*) is introduced and discussed in details since the structure of chaotic eigenstates plays a basic role in the approach. In next Section 2.4 the structure of the strength function is considered and compared with that of exact eigenstates. Main attention is paid to the conditions under which this form is the Lorentzian, and how this form changes with an increase of interaction strength. In Section 2.5 very recent analytical results are discussed, which are obtained for the shape of the strength function in the TBRI-model for any strength of interaction. Section 2.6 is devoted to non-statistical properties of this model. Specifically, it is shown that some quantities can not be described in a statistical way, in spite of completely random character of the two-body interaction.

Next Section 3.1 starts with the discussion of the basic relation between the structure of exact eigenstates and the *distribution of occupation numbers* (DON). It is shown that the average shape of eigenstates plays a crucial role for this distribution and practically determines mean values of single-particle operators. In next Section 3.2 the relevance of the DON for isolated systems, to the standard canonical distribution is discussed. It is shown how the canonical distribution emerges in isolated systems with an increase of the number of interacting particles. In next Section 3.3 the problem of the Fermi-Dirac distribution is considered for the TBRI-model of interacting Fermi-particles, in particular, conditions under which this distribution occurs in isolated systems are analyzed. An important problem of the statistical description of the occupation number distribution is considered in Section 3.4. An analytical approach has been developed in order to obtain the DON in the case of statistical equilibrium which results from the chaotic structure of eigenstates. This approach is valid even for small number of particles, in the case when the DON differs from the Fermi-Dirac distribution. In next Section 3.5 another approach is suggested for the description of the DON,

in the case when its form is of the Fermi-Dirac type. It was shown how the DON can be obtained by a proper renormalization of the total energy of a system, originated from the interaction between particles. General discussion of the meaning of temperature in isolated systems of finite number of particles is the content of Section 3.6. The main point is that for small number of particles different definitions of temperature give different results. Therefore, is it of interest to compare these definitions and to understand their meanings, if any. Finally, in Section 3.7 main results are summarized for the transition to chaos and equilibrium in the TBRI-model in dependence on the interaction strength. In last Section 4 it is briefly shown how the developed approach can be applied to dynamical systems.

II. TWO-BODY RANDOM INTERACTION MODEL

A. Description of the model

1. Many-body Hamiltonian

The model we discuss here deals with Hamiltonians which can be separated in two parts,

$$H = H_0 + V \tag{1}$$

where H_0 describes the "unperturbed " part and V stands for the interaction between particles or between different degrees of freedom. In order to study statistical properties of such models we assume in the following that the interaction is completely random. In contrast with standard approach of the RMT where matrix elements of V are taken as random variables, we would like to keep an important physical property of real systems and to take into account that the interaction is of the two-body nature. Therefore, we start with the single-particle Hamiltonian which refers n non-interacting particles occupying m single-particles levels, and assume that the matrix elements of the *two-body interaction* $V_{s_1 s_2 s_3 s_4}$ are independent random variables. Here, the indices s_1, s_2, s_3, s_4 indicate initial (s_1, s_3) and final (s_2, s_4) single-particle states coupled by the interaction.

In what follows we consider Fermi-particles, however, the approach can be easily extended to Bose-particles [17,18]. Therefore, in the Slater determinant basis the unperturbed part has simple form

$$H_0 = \sum \epsilon_s \, a_s^\dagger a_s \tag{2}$$

and the perturbation can be represented as

$$V = \frac{1}{2} \sum V_{s_1 s_2 s_3 s_4} \, a_{s_1}^\dagger a_{s_2}^\dagger a_{s_3} a_{s_4}. \tag{3}$$

Here ϵ_s is the energy of a particle, corresponding to the single-particle state $|s\rangle$ and $a_{s_j}^\dagger$, a_{s_j} are creation-annihilation operators. With these notations, exact eigenstates $|i\rangle$ of the total Hamiltonian H *(compound states)* can be expressed in terms of eigenstates k of the unperturbed part H_0 *(basis states)* as follows

$$|i\rangle = \sum_k C_k^{(i)} \, |k\rangle \, , \qquad |k\rangle = a_{s_1}^\dagger \, . \, . \, . \, a_{s_n}^\dagger \, |0\rangle \tag{4}$$

where $C_k^{(i)}$ is the $k-th$ component of the compound state $|i\rangle$ in the unperturbed basis. These components determine the important quantity which will be discussed in great details below, the *occupation numbers* n_s ,

$$n_s = \langle i| \, \hat{n}_s \, |i\rangle = \sum_k \left| C_k^{(i)} \right|^2 \langle k| \, \hat{n}_s \, |k\rangle \tag{5}$$

with $\hat{n}_s = a_s^\dagger a_s$ as the occupation number operator. For Fermi-particles the occupation number $n_s^{(k)} = \langle k| \, \hat{n}_s \, |k\rangle$ is equal to 1 or 0 depending on whether any of the particles in the basis state $|k\rangle$ occupies or not the single-particle state $|s\rangle$.

As one can see, our model is described in terms of many-particles basis states $|k\rangle$ and exact (compound) states $|i\rangle$ which are constructed from the single-particle states $|s\rangle$ and two-body matrix elements $V_{s_1 s_2 s_3 s_4}$. In what follows we assume that the basis states are reordered in an increasing way for the total energy $E_k = \sum_s \epsilon_s n_s^{(k)}$ with an increase of the index $k = 1, \ldots, N$. This way of the ordering of the unperturbed basis is crucial for the analytical description of chaotic compound states which are formed by the interaction between many basis states, see below. The size N of

the basis for the many-particles Hamiltonian H can be found from the combinatorics: if any single-particle state can be occupied by one particle only, one can get

$$N = \frac{m!}{n!(m-n)!} \sim \exp\left(n \ln n + (m-n) \ln \frac{m}{m-n}\right) \tag{6}$$

where m is the number of single-particle states (*orbitals*). The latter estimate in (6) shows that total number of many-particle states increases very fast (exponentially) with an increase of the number of particles and orbitals. For example, for $m = 11$ and $n = 4$ the size of the $H-$matrix is $N = 330$. The model with these parameters has been studied in great details in [12–15] and compared with direct computations of the Ce atom [19–21]. For this atom there are $n = 4$ valence electrons, and the core can be effectively described by the Hartree-Fock method. This method has been used [19–21] in order to calculate the basis set of single-particle relativistic states with energies ϵ_s as well as the matrix elements $V_{s_1 s_2 s_3 s_4}$ of interaction between valence electrons. The Ce atom is known to have good statistical properties, and this was the reason in [12–15] to compare direct calculations with the simplest model (1,2,3) we are going to discuss. In spite of the fact that this model does not take into account the momentum (it depends only on the energy and for this reason can be treated as "zero-dimensional ", it turns out to be instructive for the comparison of the real (*dynamical*) Ce atom with the two-body random interaction model (*TBRI-model*) described above (for details see [12–15]). In what follows, for the single-particle energies ϵ_s we take a non-degenerate spectrum with constant mean level spacing $d_0 =< \epsilon_{s+1} - \epsilon_s >$ which, without the loss of generality can be taken $d_0 = 1$. The unperturbed single-particle spectrum has been chosen at random, or according to the expression $\epsilon_s = d_0(1 + 1/s)$ (the results are statistically the same). As one can see, the model is defined by four parameters, m, n, d_0 and $V_0^2 = \left\langle V_{s_1 s_2 s_3 s_4}^{\ 2} \right\rangle$ which is the variance of two-body random matrix elements (we assume that the distribution of these elements is the Gaussian with the zero mean).

The Hamiltonian (1) with (2) and (3) is of general form, it appears in many physical applications such as when describing complex atoms, nuclei, atomic clusters etc. In fact, the form of H discussed above is known as the *mean field approximation* for complex quantum systems of interacting particles. In this description, the unperturbed part H_0 represents the zero-order mean field for the excited states with the ground state E_1, and the *residual* two-body interaction is given by V . Therefore, the single-particle levels ϵ_s in such applications are, in fact, renormalized quasi-particle energies (see details, for example, in [22]). The considered here model does not take into account such physical effects as momentum dependence, pairing effects and others, however, it contains the main effects of quantum chaos and is very effective for the understanding generic features of complex systems. Moreover, as was pointed out, the approach we discuss below, can be extended for *dynamical* quantum systems which exhibits *complex behavior*.

From the view point of dynamical systems when the complexity of the behavior appears as a result of *dynamical chaos* (both for the systems with or without *the classical limit*), the separation of the total Hamiltonian in two parts is well defined physical procedure. Specifically, the approach is expected to be valid if the second part V is as "random " as possible. In other words, one should find such separation that the perturbation has no strong regular part, the latter should be embedded into the "unperturbed " Hamiltonian H_0 . In this way, the compound states may be treated, for sufficiently strong perturbation, as chaotic superposition of simple basis states. As is well known, such a situation is typical for many-electron atoms and heavy nuclei. Indeed, the number of basis states (number N_{pc} of *principal components*) is known to be about $10^4 - 10^6$ for excited nuclei, and ~ 100 in excited rare-earth or actinide atoms.

By assuming the complete randomness of two-body elements in our models, we avoid the influence of any regular effects. Therefore, our goal is to explore statistical properties of the model in its strongest "chaotic " limit. One should stress that the answer is far from being trivial since the many-body Hamiltonian H turns out to be quite different from standard random matrix ensembles of the RMT and, as will be shown, some important quantities can not be described statistically.

It should be noted that the TBRI-model we discuss here, for the first time was analyzed long ago (see [10,11], also, the review [3] and references therein). The original interest was related to the fact that for standard random matrices the density of states has the famous *semicircle* form, in contrast with physical systems for which the RMT was addressed (complex nuclei). Moreover, the density of states for many-body systems increases very fast, and has nothing to do with the semicircle even on a local scale. Therefore, the natural question is to understand what is missed in the RMT. For this reason, another ensemble of matrices has been suggested which takes into account $k-$body interaction between particles. The theoretical study has been shown that, indeed, fully random matrices of the kind considered in the standard RMT, formally correspond to the case $k \to \infty$. On the other hand, with decrease of k , the density of states tends to the Gaussian form. The latter form is closer to reality and on a local scale, the density may be treated as the realistic one. Another question which has been under close investigation, is the role of k-body interaction on the spectrum statistics, see discussion below. For some reason, these studies have not been extended until recently, when the role of two-body interaction in different applications was questioned in the context

of quantum chaos. Unlike the previous studies, below we pay the main attention to chaotic properties of eigenstates, and to the problem of how these properties can be linked to the properties of single-particle operators, such as the *occupation number distribution*.

2. Structure of the Hamiltonian matrix

Let us start with the structure of the Hamiltonian H in the chosen basis. For this, one should construct matrix elements $H_{ij} = \langle i| H |j\rangle$ which correspond to the coupling between basis states $|i\rangle$ and $|j\rangle$ due to the interaction V. One can immediately see that the number $N_2 = m^2(m-1)^2/2$ of independent matrix elements $V_{s_1 s_2 s_3 s_4}$ of the two-body interaction is much less than the total number $N(N+1)/2$ of the (symmetric) matrix elements H_{ij} . It is very important that due to a two-body character of the interaction, the matrix elements H_{ij} are non-zero only when basis states $|i\rangle$ and $|j\rangle$ differ by no more than two occupied single-particle states. In order to count the total number K of non-zero matrix elements H_{ij} for the fixed i, we separately count the numbers K_0 , K_1 , K_2 of non-zero matrix elements which correspond to the transition between the basis states which differ by the positions of none, one and two particles, respectively,

$$K_0 = 1, \qquad K_1 = n(m-n), \quad K_2 = \frac{1}{4} n(n-1)(m-n)(m-n-1). \tag{7}$$

As a result, the total number K in each line of the matrix is

$$K = K_0 + K_1 + K_2 = 1 + n(m-n) + \frac{1}{4} n(n-1)(m-n)(m-n-1) \approx \frac{1}{4} n^2 m^2 \tag{8}$$

where the last estimate is given for large number of particles and orbitals, $1 \ll n \ll m$. Comparing K with N defined by Eq.(6) , one can see that the matrix H is *sparse* (only for $n = 2$ there is no forbidden transitions and the matrix is full).

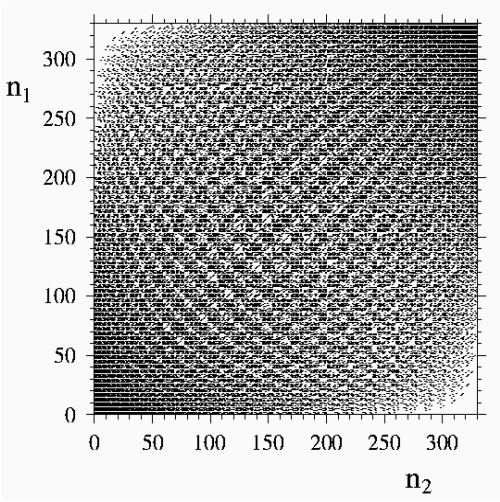

FIG. 1. Sparsity of the Hamiltonian matrix H_{n_1,n_2} for $n = 4$ particles, $m = 11$ orbitals. Black points are non-zero matrix elements.

The presence of many zeros in the matrix means that, in a sense, there are strong correlations between matrix elements since the position of zeros are fixed for any random choice of the two-body random matrix elements. It should by pointed out that the sparsity increases with an increase of the number of particles, therefore, the more particles (and orbitals), the less relative number of non-zero elements. This fact is important for the description of such systems by the random matrix approach. One should remind that in the standard RMT, the *sparsity* is not taken into account at all.

The sparsity of the matrix for $m = 11$ and $n = 4$ is shown in Fig.1 where black points correspond to non-zero elements. First, one can see that the density of zero elements increases when moving away from the principal diagonal.

Second, the positions of non-zero matrix elements are correlated, there are some curves along which the density is high, this reflects the two-body nature of interaction. In contrast with full random matrices of the standard RMT, the influence of the off-diagonal elements depends on the distance from the principal diagonal. To illustrate this peculiarity, we averaged the modulo of the off-diagonal matrix elements over blocks of the fixed size 10×10 in such a way that instead of the matrix of the size $N \times N$ we have the reduced size $N/10 \times N/10$. The result is shown in Fig.2 where only off-diagonal terms are presented. As one can see, the amplitude of these effective matrix elements decreases when moving away from the diagonal. This means that the effective intensity of the off-diagonal terms far from the diagonal is less than of those close to the diagonal. In some sense, one can treat the structure of the Hamiltonian as the *band-like*, although it is clear that the amplitude of the averaged matrix elements decays quite slowly.

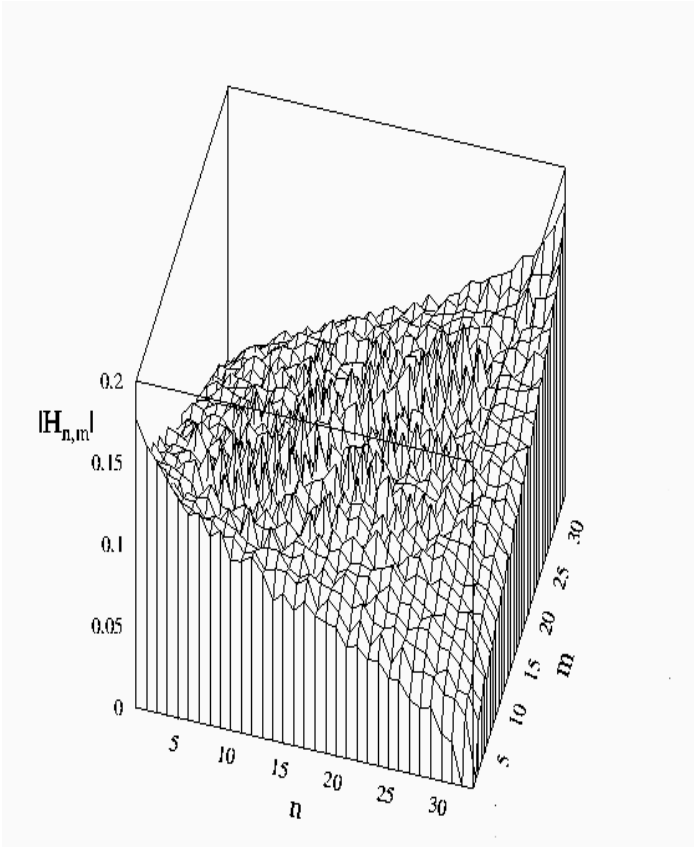

FIG. 2. Shape of the Hamiltonian matrix (without leading diagonal $H_{i,i}$). The matrix for $n = 4, m = 11, V_0 = 0.12, d_0 = 1.0$ has been divided into blocks of size 10×10 and the sum $|H_{n,m}| = \sum_{i,j} |H_{i,j}|$ has been computed inside each block (n, m) . This type of the average allows to see effective intensity of the off-diagonal matrix elements.

3. Correlations in off-diagonal matrix elements

Now, let us analyze non-zero off-diagonal elements of the matrix H_{ij} . According to the definition (3), any of these elements is just a sum of one or more two-body matrix elements. When the basis states $|i\rangle$ and $|j\rangle$ differ by one occupied orbital, $|j\rangle = a^\dagger_{s_2} a_{s_1} |i\rangle$, the matrix element H_{ij} is the sum of $n-1$ two-body matrix elements,

$$H_{ij} = \sum_{\mu}^{n-1} V_{s_1 \mu\, s_2 \mu} = \sum_{\mu \neq \alpha}^{n-2} V_{s_1 \mu\, s_2 \mu} + V_{s_1 \alpha\, s_2 \alpha} \tag{9}$$

Here the last equality is given in order to show that among other matrix elements $H_{i'j'}$ there are such elements which differ from H_{ij} by the last term only and the sum of $n-2$ is exactly the same [13],

$$H_{i'j'} = \sum_{\mu}^{n-1} V_{s_1 \mu\, s_2 \mu} = \sum_{\mu \neq \alpha}^{n-2} V_{s_1 \mu\, s_2 \mu} + V_{s_1 \beta\, s_2 \beta} \tag{10}$$

with $\alpha \neq \beta$. This happens for those basis states whose many-particle energies differ by the energy difference corresponding to the move one particle from the orbital α to the orbital β ,

$$E_{i'} - E_i = E_{j'} - E_j = \epsilon_\beta - \epsilon_\alpha \tag{11}$$

One can see that these matrix elements, strictly speaking, can not be treated as completely independent variables. Therefore, if one averages over the ensemble of matrices H_{ij} which constructed from different sets of two-body random elements, the correlations for such elements remain, $\langle H_{ij} H_{i'j'} \rangle \neq 0$.

The more striking result arises when considering matrix elements H_{ij} which correspond to the coupling between those basis states $|i\rangle$ and $|j\rangle$ which differ by two occupied orbitals, $|j\rangle = a^\dagger_{s_2} a_{s_1} |i\rangle$. These matrix elements are equal to the corresponding single two-body matrix elements, in other words, there is only one term in the sum in Eq. (3), $H_{ij} = V_{s_1 \mu_1\, s_2 \mu_2}$. These matrix elements correspond to the move of two particles from the orbitals s_1 , s_2 to other orbitals μ_1 , μ_2 . At the same time, the rest of particles ($n-2$ particles) can occupy different $m-4$ orbitals. Therefore, the same matrix element stands for other basis states $|i'\rangle$ and $|j'\rangle$ with the same move of two particles, thus, $H_{i'j'} = H_{ij} = V_{s_1 \mu_1\, s_2 \mu_2}$. As a result, among matrix elements of the Hamiltonian matrix H_{ij} there are equal matrix elements, although they are chosen randomly from the ensemble of two-body random matrices. This non-trivial fact indicates that, in spite of completely random character of the two-body interaction, the (non-zero) matrix elements of the many-body Hamiltonian are not completely independent variables!

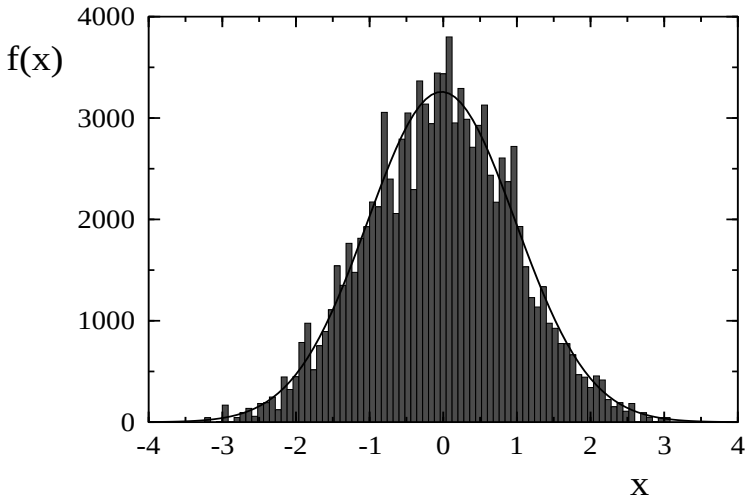

FIG. 3. Distribution of normalized off-diagonal matrix elements of the matrix $H_{i,j}$ for the parameters of Figs.1-2. Each of matrix element $H_{i,j}$ has been normalized to its variance computed from the average over $N_g = 16$ matrices with different realizations of the (random) two-body matrix elements. The smooth curve is the best fit to the Gauss which is expected for uncorrelated matrix elements.

The role of the above underlying correlations which are due to a two-body character of the interaction, is an interesting and important problem (see [13]), we will discuss some results in Section 2.6. Here, we would like to show that these correlations can be easily detected by the study of the distribution of matrix elements H_{ij} . For this, let us take the ensemble of the Hamiltonians H with different two-body random matrix elements $V_{s_1 s_2 s_3 s_4}$ keeping all other parameters. Then, for any fixed values i and j , we can find numerically the distribution of non-zero matrix elements H_{ij} . Finally, we normalize each of these distributions to their variances and make the summation. The resulting normalized distribution is shown in Fig.3. The envelope of this distribution looks like the Gaussian, however, the deviations are *non-statistical* ones which can be easily seen by the χ^2-test (for some bins of the histogram, the difference is more than 100 standard deviations).

B. Density of states and spectrum statistics

As was pointed out, the density of states $\rho(E)$ for the two-body random model was found to have the gaussian form [10,11]. Rigorous proof is given for the limit case of a very large number of particles and orbitals. However, even for relatively small values of m and n the distribution is very close to the Gaussian, see Fig.4. It is known that the density of realistic physical systems such as complex atoms and heavy nuclei can be approximated as $\rho(E) \sim \exp(A\sqrt{E-E_0})$ where E_0 is the ground energy. Therefore, the simplest model of the two-body interaction does not give exact correspondence to a real density, however, it reproduces very fast increase of the density with the energy. One should note that for full random matrices of the standard RMT, the density has the semicircle form which is very far from the reality. It is clear that in order to compare statistical properties of our Hamiltonian H_{ij} with those of complex quantum systems, one should use the left part of the energy spectrum since the decrease of the density in the right part is due to artificial cut-off of the single-particle spectrum (finite values of m).

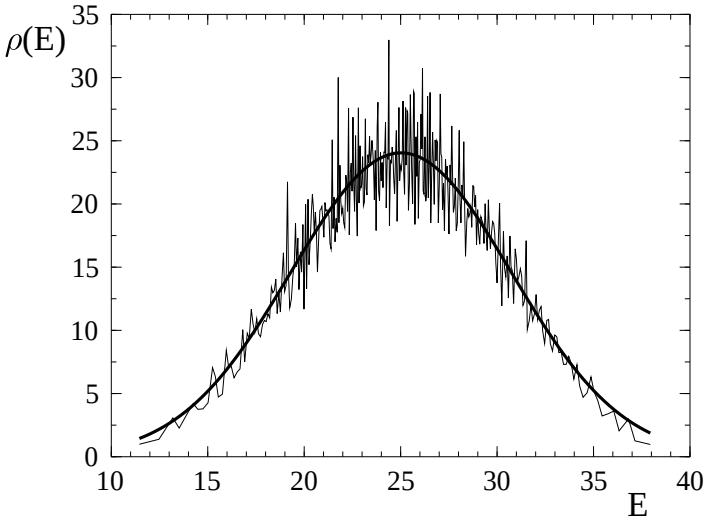

FIG. 4. Density of states of the TBRI-model with the same parameters as in Figs.1-3. The average over $N_g = 20$ is taken. The smooth curve is the best fit to the Gaussian, with $\sigma = 5.72$ and $\overline{E} = 25.1$.

The interesting question is about the type of fluctuations in the energy spectrum of the TBRI-model in comparison with those predicted by the RMT. A particular interest is the distribution of normalized spacings S between nearest energy levels. For standard random matrices the RMT reveals specific kind of the distribution known as the *Wigner-Dyson distribution*. In particular, for symmetric real random matrices (the so-called, Gaussian Orthogonal Ensemble of random matrices), the level spacing distribution $P(S)$ with a high accuracy can be described by the following form,

$$P(S) = \frac{1}{2}\pi\, S \exp\left(-\frac{\pi S^2}{4}\right) \tag{12}$$

where $\langle S\rangle = 1$. In [10,11] it was shown that for the limit case of a very strong interaction, when one can neglect the influence of the mean field (or, the same, without the leading diagonal in the Hamiltonian H_{ij}), the form of $P(s)$ turns out to be quite close to the expression (12). On the other hand, when studying the distribution of spacings between the levels E_i and E_{i+k} with $k > 1$, the difference between the result of the RMT and the TBRI-ensemble is noticeable and increases with k . This means that the level spacing distribution $P(s)$ is quite insensitive quantity of spectral correlations and does not "feel " the difference of TBRI-matrices from the full random matrices.

In physical applications, the interaction V is typically of the same order as the "unperturbed " Hamiltonian H_0 since in the mean field approximation the term H_0 absorbs regular part of the interaction and V is the (chaotic) part of the interaction which can not be included in H_0 . However, there are many cases when the interaction is weak compared to H_0 , therefore, the important question is how spectral fluctuations, in particular, the level spacing distribution, depend on the interaction and on total energy E_i . The origin of the Wigner-Dyson distribution (12) is related to the onset of chaos in the exact eigenstates (see, for example, [7]). In standard random matrices the

WD-distribution occurs for any energy since all eigenstates are completely random (their components are distributed according to the gaussian distribution for large size of the matrices).

Experimental data for complex atoms [23], [24] and heavy nuclei [25] (see also references in [6]) agree with the Wigner-Dyson statistics. The WD-distribution has been also observed in numerical calculations for the Ce atom [19–21] and the nuclear shell-model [26–28].

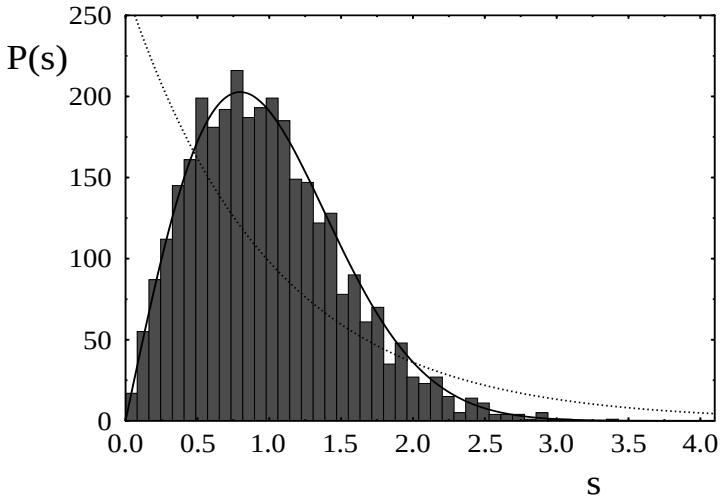

FIG. 5. Level spacing distribution for the parameters of Figs.1-3 with $N_g = 10$. All but 10 levels from both edges of the energy spectrum are taken into account, with proper rescaling to local mean level spacings. Solid curve it the Wigner-Dyson distribution and the dotted curve is the Poisson, the latter occurs for uncorrelated energy sequences.

In the TBRI-model, the randomness of the components of eigenstates is different for different eigenstates. This fact influences the spectrum statistics if one average over a large part on energy spectrum. In Fig.5 the level spacing distribution for the TBRI-model is shown for the parameters which may be compared with the Ce atom thoroughly studied in [19–21], $n = 4$, $m = 11$, $d = 0.5$, $V_0 = 0.12$. The average over $N_g = 10$ different matrices H_{ij} has been done in order to have representative statistics. All but 10 levels from the spectrum edges have been taken into account. By searching the structure of eigenstates, one can see that all eigenstates seem to be quite random (see examples below). However, one can detect clear non-statistical (regular) deviation from the WD-distribution which should be treated as quite strong, having in mind insensitive character of $P(s)$. This result may be regarded as an indication of not strong enough interaction between particles. Detailed study of the onset of the WD-distribution in the TBRI model has been recently performed in Ref. [29].

C. Structure of exact eigenstates

Our main interest in this Section is in the structure of exact eigenstates. The choice of the unperturbed basis, reordered in increasing energy, allows us to understand what happens with an increase of the interaction. In the standard perturbation theory the natural parameter which controls the intensity of the perturbation is the ratio λ of the interaction to the mean level spacing D between the unperturbed energy levels. Since the value of D is defined by the total density of states, $D = \rho^{-1}(E)$, one can expect that our control parameter is $\lambda = V_0/D$. However, in [30] it was shown that due to a two-body character of interaction, the correct parameter is different. Indeed, in the first order of the perturbation theory, the interaction couples not all unperturbed states but those basis states which correspond to the shift of not more than two particles. This means that the density of states which are coupled by the two-body interaction is much less than the total density $\rho(E)$. Therefore, the correct mean level spacing d_f that has to be compared with the interaction V_0 , is much larger than D .

If the interaction is very weak, $V_0 \ll d_f$, the standard perturbation theory can be applied. In this case any of the eigenstates in the unperturbed basis has the form of the delta-function (originated from the unperturbed state $|n_0\rangle$) plus small admixture of other components with amplitudes decreasing as $|C_n| \sim 1/|n - n_0|$, therefore, the *number of principal components* is small, $N_{pc} \sim 1$. In this case one can speak about *perturbative localization* of eigenstates

in the unperturbed basis. This situation is quite typical for eigenstates corresponding to low energies, in the energy region where the density of states is small.

With an increase of perturbation (or when passing to higher eigenstates for the fixed V_0), the number N_{pc} of principal components with essentially large amplitudes C_n increases and can be very large, $N_{pc} \gg 1$, even if V_0 is less than d_f . Such a situation occurs when $V_0 \gg \frac{1}{\pi^2}\sqrt{D\, d_f}$, see details in [15]. In such a case the structure of eigenstates is "chaotic ", however, there are many "holes " inside such eigenstates in a given basis. Therefore, in spite of large number of components, these *sparse eigenstates* are non-ergodic, which leads to *non-gaussian statistics*. Namely, the fluctuations of the components C_n can be extremely large and statistical description is not valid. One should stress that in this case the number of principal components can not be estimated as $N_{pc} \approx \Gamma/D$, as is typically assumed in the literature (here Γ is an effective "size " of the eigenstates in unperturbed energy representation, see below).

When the interaction is relatively strong, $V_0 \approx d_f$, specific transition occurs from non-ergodic to ergodic eigenstates. This transition has been discovered in [30] by considering the flow of the energy in the Fock-space of excited states. For very large number of particles this transition is sharp and may be compared with the Anderson transition in solid state models (see for example details in [30,31]). Therefore, the condition $V_0 > d_f$ can be considered as the transition to chaos inside compound eigenstates, thus, allowing to describe the model in a statistical way, see below. An example of such chaotic eigenstates is given in Fig.6 for the parameters related to the Ce atom. One can see that for large excitation energy (n is the number of exact eigenstates reordered in increasing energy $E^{(n)}$), the eigenstates look more extended (delocalized) in the unperturbed basis. It is interesting to note that they look very similar to the eigenstates of the Ce atom, obtained in the direct quantum computation based on the Hartree-Fock method [19–21]. For the first time, chaotic structure of eigenstates of the Ce atom has been revealed in [32].

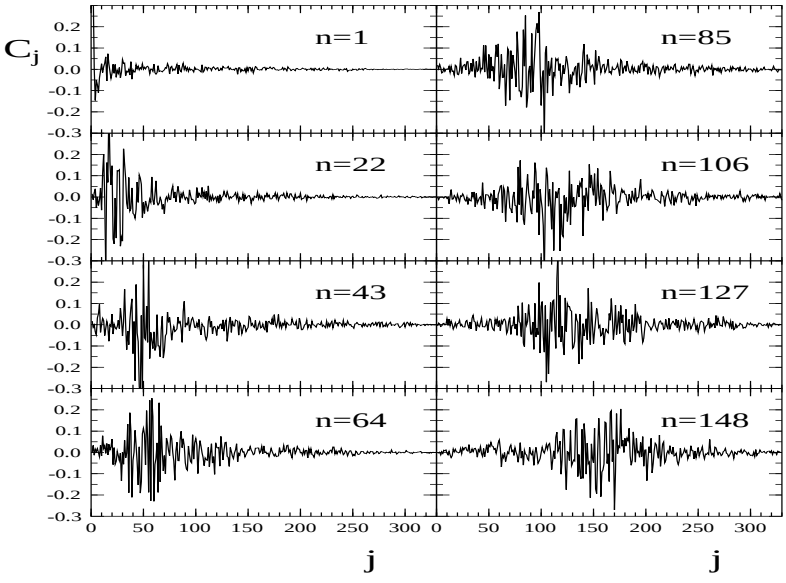

FIG. 6. Examples of the exact eigenstates of a matrix H_{ij} for the same parameters as in the previous figures. Components C_j of 8 eigenstates for exact eigenstates in the low part of the spectrum are shown.

Let us now discuss how to quantitatively characterize chaotic eigenstates. First, we introduce the matrix

$$w_j^{(n)} \equiv \left|C_j^{(n)}\right|^2 = \left|C_j(E^{(n)})\right|^2 \tag{13}$$

constructed from the exact eigenstates $|n\rangle$ corresponding to the energy $E^{(n)}$. In what follows, we use the notations which refer low indices to the basis states, and upper indices to the exact (compound) eigenstates. Thus, the structure of eigenstates is given by the dependence $w_j^{(n)}$ on j for fixed values of n . On the other hand, if we fix the index j and explore the dependence $w_j^{(n)}$ on n , one can understand how the unperturbed state $|j\rangle$ is coupled to other basis states due to the interaction. The latter quantity is very important since it gives the information about the spread of the energy, initially concentrated in a specific basis state $|j\rangle$, when switching on the interaction. The envelope of

this function $w_j^{(n)}$ in the energy representation is known as *strength function* or *local spectral density of states* (LDOS) and will be discussed in details in next Section.

From Fig.6 one can conclude that when the number of principal components is large, $N_{pc} \gg 1$, such eigenstates may be treated as random superposition of components $C_j^{(n)}$, although they do not occupy the whole unperturbed basis. The gaussian character of the fluctuations of $C_j^{(n)}$ depending on the indices j or n , has been revealed in [19–21] for the Ce atom, thus allowing to treat the exact eigenstates of a dynamical systems, as *chaotic eigenstates*.

The size of the basis which they occupy can be associated with the "size " of eigenstates, or, with the *localization length*. As is known, the notion of the localization length is very important in solid state applications, when studying the eigenstates of disordered models in infinite basis in the position representation. In such applications the localization length l_∞ is defined via exponential decrease of the square of the amplitude of eigenstates . For the finite basis, the definition of the localization length can be generalized in a way described in [7]. Following to [7,8] we define here two localization lengths, namely, the "*entropy localization length*" l_h, and the localization length l_{ipr} associated with the so-called *participation ratio*. The first one is defined by the expression

$$l_h = N \exp(\langle \mathcal{H} \rangle - \mathcal{H}_0), \tag{14}$$

where $\langle \mathcal{H} \rangle$ is the mean " *entropy*" of eigenstates,

$$\langle \mathcal{H} \rangle = -\frac{1}{M} \sum_{n=1}^{M} \sum_{j=1}^{N} w_j^{(n)} \ln (w_j^{(n)}) \tag{15}$$

and $\mathcal{H}_0$ is the normalization constant which is equal approximately to 2.08 in the case of pure gaussian fluctuations of C_j (see details e.g. in [7]). Here M is the number of eigenstates which are taken for the average. This can be the number of eigenstates of one matrix H_{ij} taken from a small energy window, or the number of eigenstates for the fixed n , computed from different matrices H_{ij} with different realization of disorder in two-body matrix elements.

The second definition is commonly used in solid state applications (see e.g. [8]). Assuming the gaussian character of fluctuations of the components of eigenstates, the localization length l_{ipr} is defined by

$$l_{ipr} = \frac{3}{P}; \qquad P = \frac{1}{M} \sum_{n=1}^{M} \sum_{j=1}^{N} \left(w_j^{(n)} \right)^2 \tag{16}$$

In the above expressions (14, 16) the factors 2.08 and 3 are, in fact, normalizing coefficients which provide, in the limit case of completely extended and gaussian eigenstates in the finite basis of the size N , the "maximal" value of the localization length $l_h = l_{ipr} = N$. In other extreme case of a strong (exponential) localization in the unperturbed basis, the above two localization lengths are proportional to that found from the tails of eigenstates (see [7]). The dependence of the localization lengths l_h and l_{ipr} on the basis number and energy of exact eigenstates is given in Fig.7a-b. The average over $N_g = 50$ matrices H_{ij} with different realizations of two-body matrix elements has been taken, in order to smooth strong fluctuations in the value of localization lengths of individual eigenstates. The above definitions of localization length can be taken for the estimate of a number of principal components N_{pc} , and can be associated with the degree of "chaoticity " of compound eigenstates. The data of Fig.7 show quite good correspondence with direct computations [19,20] performed for the Ce atom, for which the localization length l_h was found to be about $l_h \approx 110 - 130$. Comparing Fig.7b with Fig.4 of the density of states $\rho\,(E)$, one can see the similarity. This fact can be understood from the simplest estimate of N_{pc} as a total number of (basis) states defined by the "width" Γ , the latter can be approximated as the mean-square-root of the distribution $w_j^{(n)}$ for the fixed n ,

$$N_{pc} \approx \frac{\Gamma}{D} = \Gamma \rho\,(E) \tag{17}$$

One should stress that this expression is valid for ergodic eigenstates ($V_0 \geq d_f$) and shows the proportionality of N_{pc} to the density. As for the width Γ , it is approximately independent of the excitation energy, see below.

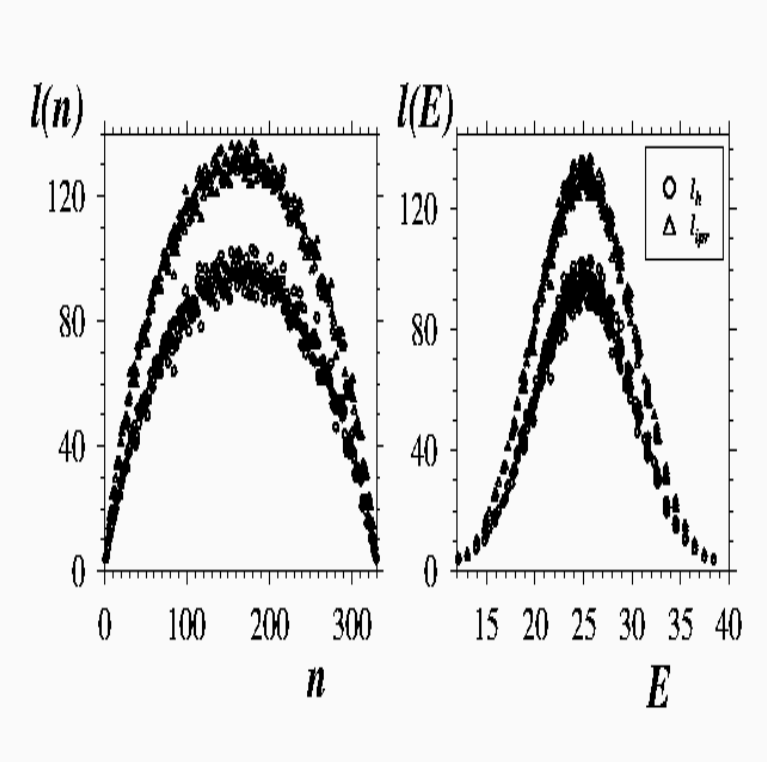

FIG. 7. (a) Localization lengths l_h and l_{ipr} are given in dependence on the number n of exact eigenstates $|n\rangle$, see (14) and (16). The parameters are taken the same as in Figs.1-6, with $N_g = 50$. (b) the same as in (a), but in the energy representation.

Eq.(15) reflects general relation between the number of principal components N_{pc} and the *entropy of eigenstates*,

$$S_{EF} = \ln N_{pc} \tag{18}$$

where S_{EF} stands for any reasonable definition of the entropy. In application to shell models of complex nuclei this relation has been studied in great details in [26,28]. Combining Eq.(18) with Eq.(17), one can get

$$S_{EF} \approx \ln \rho(E) + \ln \Gamma(E) \tag{19}$$

In contrast to the density of states, the width Γ is a weakly dependent function of the energy. Therefore, the entropy S_{EF} found from exact eigenstates practically coincides with the thermodynamical entropy, the fact which was mentioned for the first time in [26,28].

D. Strength function

In this Section we discuss the properties of the *strength function* which is defined as

$$W(E^{(m)}, j) = \sum_n |C_j^{(n)}|^2 \delta(E - E^{(n)}) \tag{20}$$

Here $C_j^{(n)}$ are the components of eigenstates $|n\rangle$ ("compound" states) of the total Hamiltonian H given in the unperturbed basis $|j\rangle$, and $E^{(n)}$ is the energy associated with the state $|n\rangle$. The sum is taken over a number of eigenstates $|n\rangle$ chosen from a small energy window centered at the energy $E^{(m)}$. One can see that this function $W(E, j)$ is originated from the same matrix $w_j^{(n)}$ which has been introduced in previous Section when discussing the structure of exact eigenstates. Indeed, an exact eigenstate is characterized by the dependence $w_j^{(n)}$ on j for the fixed value n (associated with the energy $E^{(n)}$). On the other hand, the strength function is characterized by the same

function $w_j^{(n)}$ when index j is fixed and we are interested in the dependence on the energy $E^{(m)}$ due to the relation between $E^{(n)}$ and n therefore,

$$W(E^{(m)},j) \simeq F_j^{(n)}\rho(E), \qquad F_j^{(n)} \equiv \overline{w_j^{(n)}}. \tag{21}$$

Here we have introduced the *F−function* $F_j^{(n)}$ which gives the envelope of $w_j^{(n)}$ in dependence on the indices j and n (the bar stands for the average inside small windows centered at j and n). In fact, the strength function is the (smooth) representation of a (simple) basis state $|j\rangle$ in terms of exact eigenstates. This function is very important since it can be measured experimentally. It contains an information about the internal interaction between unperturbed states. Namely, it shows how the unperturbed state $|j\rangle$ is coupled to the exact states $|n\rangle$ due to the interaction. An effective width of this function (*spreading width*) defines the energy range associated with the "life time" of an unperturbed state $|n\rangle$ if initially one excites specific basis state.

In solid state models the role of the unperturbed energy in Eq.(20) plays the position j of an electron and the function $W(E^{(m)},j) \Rightarrow W(E,j)$ has the meaning of the electron density of states for the fixed position j . For this reason this function is known in solid state physics as the *local density of states* (LDOS). One can see that if (apart from fluctuations) $w_j^{(n)}$ is independent of the position (or, in our application, the energy of compound state), it reduces to the total density of states, $W(E^{(m)},j) \Rightarrow \rho(E)$. Also, if the total density of states is constant, $\rho = \alpha^{-1}$, the dependence of the LDOS on j is of the form $W(E,n) = W(E-\alpha j)$. This means that the form of the LDOS is the same for any j . In our case of strong dependence of the density of states on the energy, the form of the LDOS is quite complicated, see next Section. Normalized to the mean energy level spacing, the strength function $W(E^{(m)},j)$ determines an effective number N_{pc} of principal components of compound states $|n\rangle$ which are present in the basis state $|j\rangle$.

Similar to the analysis of the structure of the eigenstates in dependence on the interaction, one can understand that for a very weak interaction $V_0 \ll d_f$ the LDOS is a delta-like function with a very small admixture of other components which can be found by the standard perturbation theory. With an increase of the interaction, the number of principal components increases and can be very large. However, if the interaction is not strong enough [15] ,

$$1 \gg \frac{V_0}{d_f} \gg \frac{1}{\pi^2}\sqrt{\frac{D}{d_f}} \ , \tag{22}$$

the LDOS is sparsed, with extremely large fluctuations of components, see details in Ref. [31]. In order to have ergodic LDOS, one needs to have the perturbation large enough, $V_0 \gg d_f$ (for a large number of particles this transition is sharp and, in fact, one needs the weaker condition, $V_0 \geq d_f$, see details in [15]).

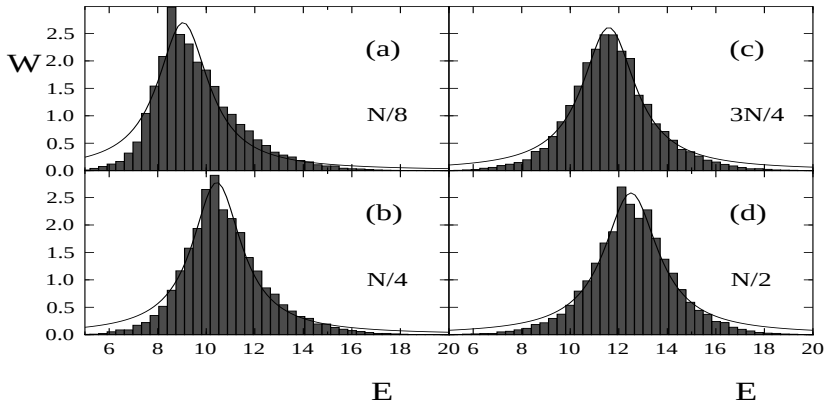

FIG. 8. Few examples of the LDOS for the TBRI-model for different basis states $j = N/8,\ N/4,\ 3N/4, N/2$. The average is done over a number of eigenstates with close energies, for $n = 4$ particles, $m = 11$ orbitals, $V_0 = 0.12, d_0 = 0.5$ and with additional average over $N_g = 50$ matrices H_{ij} . Smooth curves are the best fit to the Gaussian at the center of the energy spectrum, $j = N/2$.

For $V_0 \gg d_f$ the LDOS turns out to be ergodic and thransition to chaos occurs [30,33,31,34,29,35–37], therefore, statistical description of the model is valid. Few examples of the LDOS for the TBRI-model are given in Fig.8 for the parameters of the Ce atom. One can see strong dependence of the shape of the LDOS on the position of basis state $|j\rangle$ in the energy spectrum.

Before we start with the discussion of analytical results, it is important to point out the correspondence between the shape of the LDOS, and that of exact eigenstates which have been discussed in previous Section. Specifically, from the analysis of the structure of the eigenstate matrix $w_j^{(n)}$ one can expect the similarity between the LDOS and shape of the eigenstates. For the first time such a similarity has been observed when studying band random matrix ensembles [38,39]. Moreover, the detailed study of some dynamical models [17,40] have revealed that even when the shapes of the LDOS and EFs seem to be completely different, after a proper rescaling which involves both unperturbed and perturbed energy spectrum, both shapes are very similar. In order to compare characteristics of the LDOS and EFs, in Fig.9 the dependence of the entropy localization length on the energy is shown for both the LDOS and EFs. Apart from strong fluctuations (which are due to a chaotic nature of the components $C_j^{(n)}$), in general, the dependencies $l_H\,(E)$ look very similar.

The problem of the correspondence between shapes of the LDOS and EFs is still open, however, from the studies made up to now (see also [17,40]), one can conclude that if the width of the perturbed spectrum is of the same order as the unperturbed one (or, the same, the perturbation is not very larger), one can expect that both shapes are very close to each other. The importance of this problem of similarity for the shapes of the LDOS and EFs will be clear in next Section when we discuss the relation between the shape of the EF and generic properties of the occupation number distribution.

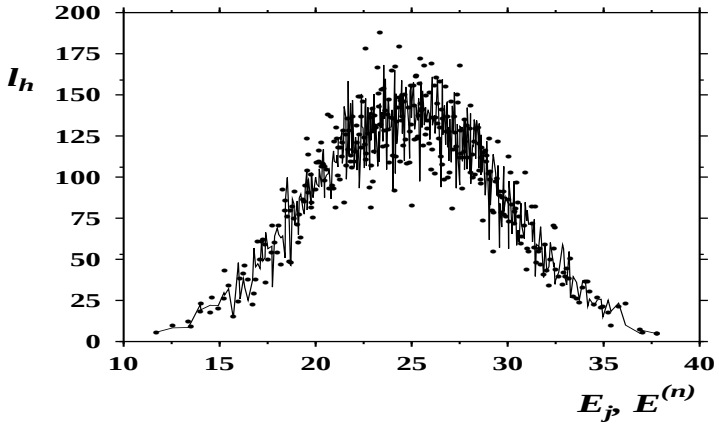

FIG. 9. Comparison of the localization length l_h for the LDOS (points) and eigenstates (line). The data are given for one Hamiltonian matrix with the same parameters as in Figs.1-7, for the same numbers $j = n$.

For the first time the form of the LDOS in random matrix theory has been discussed in Ref. [9] where band random matrix ensemble has been considered. The matrices were assumed to consist of the diagonal part H_0 in the form of reordered numbers $H_{jj} = j\,D$ (thus, the unperturbed level density is constant, $\rho_0 = D^{-1}$), and the perturbation V_0 with the random independent off-diagonal matrix elements for $|i - j| \leq b$. Outside the band of size $b \gg 1$ matrix elements are zeros. The distribution of the off-diagonal matrix elements is characterized by the zero mean, $\langle H_{ij}\rangle = 0$ and the variance $V_0^2 = \langle H_{ij}^2\rangle$. For this model, the relevant parameter was found to be

$$q = \frac{\rho_0^2 V_0^2}{b}. \tag{23}$$

Wigner analytically proved [9] that for relatively strong perturbation, $V_0 \gg D$ in the limit $q \ll 1$ (when the influence of the main diagonal H_{jj} is strong) the form of the LDOS is the Lorentzian,

$$W_{BW}\,(\tilde{E}) = \frac{1}{2\pi}\,\frac{\Gamma_{BW}}{\tilde{E}^2 + \frac{\Gamma_{BW}^2}{4}}, \qquad \tilde{E} = E - D\,n \tag{24}$$

which is nowadays known as the *Breit-Wigner* (BW) form. Here Γ_{BW} is the spreading width which is half-width of the distribution (24),

$$\Gamma_{BW} = 2\pi\rho_0 V_0^2 \tag{25}$$

and the energy $\tilde{E} = E - D\,n$ refers to the center of the distribution. In other limit $q \gg 1$ the influence of the unperturbed part H_0 can be neglected and the shape of the LDOS tends to the shape of the total density of states of band random matrices without the leading diagonal H_{jj}, which is the semicircle.

Recently, the shape of the LDOS has been studied rigorously for a more general distribution of the off-diagonal elements v_{nm} in the Wigner band random matrix model (WBRM). Namely, the variance of random matrix elements is taken to depend on the distance $r = |n - m|$ from the principal diagonal according to an envelope function $f(r)$ which, for $r \to \infty$, decreases sufficiently fast (see details in [41]). In this case the effective band size b is defined by the second moment of the function $f(r)$. Another important generalization of Ref. [41] is related to the sparsity inside the band, which can be defined as a relative number of zero elements in each line of the matrix. As was shown above, such a sparsity, which is due to the two-body nature of the interaction between the particles, is important for statistical properties of compound states.

The BW-form of the LDOS also occurs in a more general model describing the interaction of an unperturbed state with a large set of complex states, see details in the book [42]. It also appears for dynamical systems with complex behavior, such as the Ce atom [19–21], the sd shell model [26–28], as well as in random models in application to solid state physics [43,44].

For a long time it was believed that the LDOS for complex physical systems has the universal energy dependence described by the BW-distribution (24). However, when studying the structure of the LDOS and EFs of the Ce atom, it was observed some deviation from the BW-shape for large distance from the center. By applying the WBRM, in [19] it was analytically shown that the shape of the LDOS is highly non-universal for energies larger than the effective size of the band in the energy representation, $|E| \gg D\,b$ (in what follows by E we mean the distance from the center E_c of the distribution, $\tilde{E} \Rightarrow E$), see also numerical data in [41]. Namely, outside this range, the tails of the LDOS are highly non-trivial, decaying very fast (even faster than the exponent) when $|E| \to \infty$. Therefore, the range of parameters for which the form of LDOS has the BW-form in the WBRM-model, is given by the condition [41] which can be written as

$$\rho_0^{-1} \ll \Gamma_{BW} \ll b\rho_0^{-1} \tag{26}$$

Here, the left-hand-side of the inequality is related to non-perturbative character of the coupling since the perturbation should couple many unperturbed states.

The condition (26) turns out to be of generic and can be applied to real physical systems. Moreover, it can be used to find the effective band-width b_{eff} of interaction when other definitions of b are obscure. In the TBRI-model with many interacting particles the band-width is very large (practically it is infinite), and does not play any role in many solid state applications. On the contrary, in application to complex atoms and nuclei, the number of particles above the Fermi level is relatively small (four particles in the Ce atom and 12 particles in the sd shell models), and this effect can be important. It should be pointed out that the BW-dependence has infinite second moment. At the same time, in any physical application the second moment is always finite and is defined by the sum of the square of the off-diagonal elements. This fact results in non-Lorentzian tails of the LDOS.

The important question is about the shape of the LDOS for a strong interaction, when the condition (26) violates, $\Gamma_{BW} \approx b\rho_0^{-1}$. Since in the mean field approximation the "regular " part of the interaction is included in the mean field, very often the interaction V is compared with the unperturbed part H_0 . Therefore, this situation when the shape of the LDOS is very different from the BW-form, is quite physical. In order to understand what happens in this case, it is useful to study how the transition from the BW-form to the semicircle occurs in the WBRM-model. As was pointed out, the semicircle form itself is unphysical and appears when neglecting the unperturbed part H_0 . However, the form of the LDOS in the transition region seems to be of quite generic.

Numerical data in Refs. [41], [45] for the WBRM-model have shown that for the case when $\Gamma_{BW} \approx b\rho_0^{-1}$ the form of the LDOS can be approximately described by the Gaussian. The same fact has been observed and discussed in Refs. [26,28] when studying eigenstates and LDOS for shell model of nuclei. Since in the latter application the band size of the interaction is not well defined, it is better to introduce one more parameter, in addition to the half-width Γ_{BW} . As was shown in Ref. [45], in general, the form of the LDOS can be effectively described by two independent parameters, Γ_{BW} and ΔE where the latter is defined via the variance of the LDOS,

$$(\Delta E)^2 = 4\sigma_W^2 = 4\int (E - E_c)^2\, W_{BW}(E)\, dE \tag{27}$$

In the symmetric case (in the TBRI-model, at the center of the spectrum), E_c coincides with the unperturbed energy, $E = E_j$.

Then, if the parameter Γ_{BW} is much less than ΔE , the shape $W\left(E\right)$ of the LDOS is the BW-dependence (24) and Γ_{BW} has the meaning of the half-width of the distribution $W(E) = W_{BW}\left(E\right)$. On the other hand, if $\Gamma_{BW} \approx \Delta E$, the form of the LDOS is approximately the Gaussian,

$$W(E) = \frac{1}{\sigma_W \sqrt{2\pi}} \exp\left(-\frac{\left(E - E_c\right)^2}{2\left(\sigma_W\right)^2} \right) \tag{28}$$

Detailed numerical study [45] of the form of the LDOS in the region $\Gamma_{BW} \approx \Delta E$ have shown that the LDOS coincides with the Gaussian with a very high accuracy. It is important to stress that in this case, the parameter Γ_{BW} has nothing to do with the half-width Γ_{hw} of the LDOS, the latter is proportional to the mean-square-root σ_W of the Gaussian, $\Gamma_{hw} \approx C_0\, \sigma_W$ (see also discussion in [26,28]). Note that the Gaussian form typically occurs in "statistical spectroscopy" [10,46,47] when neglecting the mean field term H_0 in Eq.(1). One should note that sometimes the fact that the LDOS can deviate from the BW-form due to the influence of the finiteness of ΔE , is missing in the literature.

It is important that the center and variance of the LDOS can be explicitly expressed via diagonal and off-diagonal matrix elements respectively [15]. Indeed, the center is defined by

$$E_c = \left(\overline{E^{(n)}}\right)_j = \sum_n E^{(n)} F_j^{(n)} \approx \sum_n E^{(n)} w_j^{(n)} =$$

$$\sum_{n,m} \langle j|\, n\rangle \, \langle n|\, H\, |m\rangle \, \langle m|\, j\rangle = H_{jj} = E_j \tag{29}$$

where the relation $\langle i|\, H\, |j\rangle = \delta_{ij}\, \langle i|\, H\, |j\rangle$ is used for exact eigenstates. Correspondingly, the variance can be obtained from the matrix elements of H^2 ,

$$\left(\sigma_W^2\right)_j = \sum_n \left(E^{(n)} - E_j\right)^2 F_j^{(n)} \approx \sum_n \left(E^{(n)} - E_j\right)^2 w_j^{(n)} = \sum_{p \neq j} H_{jp}^2 \tag{30}$$

For the TBRI-model the sum of the off-diagonal elements for any fixed value of p can be evaluated exactly [13],

$$\frac{\left(\Delta E\right)_j^2}{4} = \sum_{p \neq j} H_{jp}^2 = V_0^2\, (n-1)\, K_1 + V_0^2\, K_2 = \frac{1}{4} V_0^2\, n\, (n-1)\, (m-n)\, (3+m-n) \tag{31}$$

where the expressions (7) have been used for K_1 and K_2 , and V_0^2 is the variance of the off-diagonal matrix elements. One can see that with an increase of the interaction, the half-width of the LDOS changes from the quadratic dependence $\Gamma_{hw} \sim V_0^2$ to the linear one, $\Gamma_{hw} \sim V_0$. It is interesting to note that the variance of the LDOS for Fermi-particles does not depend on the index j which stands for a specific basis state, therefore, $\left(\Delta E\right)_j^2 \Rightarrow \left(\Delta E\right)^2$

E. Analytical solution for the LDOS

Very recently, the form of the LDOS for the TBRI-model has been analytically found in [16] for any strength of perturbation. In this Section we discuss the approach of [16] and the obtained results. We would like to stress that our aim is to find the LDOS in terms of matrix elements of the total Hamiltonian H_{ij} , without its diagonalization. To start with, let us rewrite the general expression for the LDOS in the form

$$W_k\left(E\right) = F(E_k, E)\, \rho(E) \tag{32}$$

where E is the total energy of the system (energy of an exact eigenstate). As was pointed out, the $F-$function gives the shapes of both exact eigenstates and strength functions depending on what is fixed, the total energy $E \equiv E^{(i)}$ or the unperturbed one, E_k. The method used in [16] is an extension of the approach developed in [42,48], which takes into account specific structure of the Hamiltonian TBRI-matrix. Specifically, first, we fix some basis component $|k\rangle$ and diagonalize the Hamiltonian matrix without this component. Then the problem is reduced to the interaction of this component with exact eigenstates $|i\rangle$ which are statistically described by the matrix components V_{ki}. In the spirit of the approach of Ref. [42] let us introduce a small energy window Δ which will be used for an average over the total energy inside this interval. As a result, the set of equations for the LDOS can be written in the following form,

$$W_k(E) = \frac{1}{2\pi} \frac{\Gamma_k(E)}{(E_k + \delta_k - E)^2 + \frac{1}{4}\Gamma_k^2(E)} \tag{33}$$

where

$$\Gamma_k(E) \simeq 2\pi \overline{|V_{ki}|^2} \rho(E) \tag{34}$$

is some function which can be associated with the half-width of the distribution $W_k(E)$, for the case when the energy dependence is weak, $\Gamma_k(E) \simeq const$. The energy shift δ_k for the basis state $|k\rangle$,

$$\delta_k = \sum_i \frac{|V_{ki}|^2 (E - E^{(i)})}{(E - E^{(i)})^2 + \frac{\Delta^2}{4}} \tag{35}$$

is due to the asymmetry of the perturbation, if the energy E_k is not at the center of the spectrum. This shift is just the modified second order correction to the unperturbed energy level. For the calculation of the shape of the eigenvector $|i>$ one should substitute the exact energy $E = E^{(i)} = E_i + \delta_i$. Then, if the interaction is not very strong, in the evaluation of the above equations the difference $\delta_i - \delta_k$ can be neglected.

One should stress that the summation in the above equations is performed over exact states. Since the exact eigenstates are unknown, one should express everything in terms of the basis states only. To do this, we express exact eigenstates $|i>$ through the basis components,

$$|V_{ki}|^2 = \sum_p \left| C_p^{(i)} \right|^2 |H_{kp}|^2 + \sum_{p \neq q} C_q^{(i)*} C_p^{(i)} H_{kp} H_{qk} \tag{36}$$

In previous Sections it was argued that for large number of principal components, $N_{pc} \gg 1$ and sufficiently strong interaction $V_0 \geq d_f$, the components $C_{p,q}^{(i)}$ can be treated as random variables, therefore, the second term in (36) vanishes after averaging. Substitution of Eq. (36) into Eqs.(34, 35) gives

$$\Gamma_k(E) = 2\pi \sum_{p \neq k} |H_{kp}|^2 W_p(E) = \sum_{p \neq k} |H_{kp}|^2 \frac{\Gamma_p(E)}{(E_p + \delta_p - E)^2 + \frac{\Gamma_p^2(E)}{4}} \tag{37}$$

$$\delta_k = \sum_{p \neq k} |H_{kp}|^2 \int dE^{(i)} \frac{W_p(E^{(i)})}{E - E^{(i)}} \simeq \sum_{p \neq k} \frac{|H_{kp}|^2 (E - E_p - \delta_p)}{(E - E_p - \delta_p)^2 + \frac{\Gamma_p^2(E)}{4}} \tag{38}$$

where the integral is taken as the principal value. Last equality is valid in the approximation of slow variation of $\Gamma_p(E)$ and δ_p. The equations for $\Gamma_k(E)$ and δ_k allow to calculate the strength function (33) from the unperturbed energy spectrum and matrix elements of the total Hamiltonian H.

Now we have the set of equations (33,37,38) which, in principal, give the solution for the LDOS $W_k(E)$ and can be solved numerically. However, for relatively large number of particles (practically, for $n \geq 4$), one can find an approximate analytical solution of the problem [16]. By analyzing these equations, in [16] it was proved that the condition of the self-consistent solution for the LDOS (or the same, when the shape of the LDOS exists as a smooth function of the energy), is just the condition for the onset of chaos in the TBRI-model, $V_0 \geq d_f$, discussed in previous Sections.

More specifically, for a very strong interaction, $\Gamma >> d_f$ the number N_f of effectively large terms in the sums is large, $N_f \sim \Gamma/d_f$, fluctuations of Γ are small, $\delta\Gamma \sim \Gamma/\sqrt{N_f}$ and Eq. (37) can be written in the form,

$$\Gamma_k(E) \simeq 2\pi \overline{|H_{kp}|^2} \rho_f(\tilde{E}) \tag{39}$$

Here $\tilde{E} = E - \delta$ and the energy shift $\delta \equiv < \delta_p >$ can be neglected in the case of $\Gamma << \sigma$ with σ standing for an effective band-width σ of the Hamiltonian matrix H_{pq} (see Eq.(41)). In order to perform the summation over p, it was assumed that $\Gamma(E)$ and $\rho_f(E)$ change slowly within the energy interval of the size Γ. As a result, in order to have large number of final states $N_f \sim 2\pi H_{kp}^2/d_f^2$ and *statistical equilibrium* (small fluctuations of Γ), one needs $H_{kp} >> d_f$. In this case chaotic components of exact eigenfunctions in the unperturbed many-particle basis ergodically fill the whole energy shell of the width Γ, with Gaussian fluctuations of the coefficients $C_k^{(i)}$ and the variance given by the $F-$function (21) (see also [42,19,21]).

With a decrease of the ratio H_{kp}/d_f , the fluctuations of Γ increase and for $H_{kp} < d_f$ the smooth self-consistent solution of Eqs.(37) does not exist. Indeed, in this case the term Γ_p in the denominator of Eq.(37,38) can be neglected and the sum in (37) is dominated by one term with the minimal energy $E - E_p \sim d_f$. Therefore, for a typical basis state $|k>$ formally one gets $\Gamma_k \sim \Gamma_p (H_{kp}/d_f)^2 << \Gamma_p$. This contradicts to the assumption of the equilibrium according to which all components are of the same order, $\Gamma_k \sim \Gamma_p$.

One should stress again that the absence of a smooth solution for the shape of the eigenstates and the strength function does not mean that the number of principal components N_{pc} in exact eigenstates is small. It can be large, however, the distribution of the components is not ergodic, there are many "holes" inside exact eigenstates which occupy the energy shell of the width $2\pi\overline{|H_{kp}|^2}\rho_f(E)$ (see [30,15]). In such a situation, the fluctuations of $C_k^{(,i)}$ are very large and non-Gaussian.

It is important to note that the ensemble average (over many matrices H_{kp}) in this problem is not equivalent to the energy average (inside specific Hamiltonian matrix). Indeed, the average over the single-particle spectrum leads to the variation of energy denominators in (37) and can fill the "holes " in the $F-$function.

From general equations for the shape of the LDOS one can make an unexpected conclusion that the spreading width $\Gamma(E)$ can be a strong function of excitation energy E due to the variation of the density $\rho_f\,(E) = d_f^{-1}$ of final states in Eq. (39). In Ref. [16] it was shown that for the excited states, well above the ground state, the energy dependence of $\rho_f\,(E)$ and $\Gamma(E)$ can be quite close to the Gaussian. This result is based on the estimate of the two-body density $\rho_f\,(E)$,

$$\rho_f\,(E) = \rho_f^{(1)}(E) + \rho_f^{(2)}(E) \tag{40}$$

where the density ρ_f is determined by the energy difference $\omega_{pk}^{(2)}$ between the states $|p>$ and $|k>$ which differ by the position of two particles, and by $\omega_{pk}^{(1)}$ between those states which differ by the position of one particle. Detailed analysis [16] have shown that both $\rho_f^{(1)}(E)$ and $\rho_f^{(2)}(E)$ for large number of particles are described by the Gaussian,

$$\rho_f^{(1,2)}(\tilde{E}) \simeq \frac{K_{1,2}}{\sigma_{1,2}\sqrt{2\pi}}\, exp\left(-\frac{\left(\tilde{E} - E_k - \overline{\omega^{(1,2)}}\right)^2}{2\sigma_{1,2}^2}\right) \tag{41}$$

Normalization parameter $K_{1,2}$ stands for the number of one or two-particle transitions, see Eq.(7). Here the average frequency of one and two-particle transitions reads as

$$\overline{\omega^{(1)}} \approx m/(m-n)(\overline{\epsilon} - E_k/n) \tag{42}$$

and

$$\overline{\omega^{(2)}} = 2(\overline{\epsilon_p} - \overline{\epsilon_k}) \approx 2m/(m-n)(\overline{\epsilon} - E_k/n) \tag{43}$$

where $\overline{\epsilon_k} = E_k/n$ is the mean single-particle energy in the basis state $|k>$ containing n particles, $\overline{\epsilon}$ is the single-particle energy averaged over all m orbitals, and the mean energy of the empty orbitals $\overline{\epsilon_p}$ can be found from the relation $m\overline{\epsilon} = \overline{\epsilon_k}n + \overline{\epsilon_p}(m-n)$.

The variance of $\rho_f^{(1,2)}(E)$ for one and two-particle transitions is

$$\sigma_1^2 = \sigma_p^2 + \sigma_k^2 + 2(n-1)V^2 \approx \sigma_\epsilon^2 + 2(n-1)V^2 \tag{44}$$

and

$$\sigma_2^2 = 2\sigma_p^2 + 2\sigma_k^2 + (4n-6)V_0^2 \approx 2\sigma_\epsilon^2 + (4n-6)V_0^2 \tag{45}$$

where σ_ϵ^2 is the variance of single-particle spectrum, and V_0^2 is the variance of non-diagonal matrix elements of the residual interaction. Note that in the case of $n << m$ for low-lying states the variance of the occupied orbital energies σ_k^2 is small and the variance of empty orbital energies is $\sigma_p^2 \sim \sigma_\epsilon^2$.

Thus, the width $\Gamma(E)$ is given by the following expression,

$$\Gamma(E) = 2\pi\,\left[(n-1)V^2\rho_f^{(1)}(E) + V^2\rho_f^{(2)}(E)\right] \tag{46}$$

The factor $n-1$ appears since for single-particle transitions the summation in $H_{kp} = \sum_\nu V_{\alpha\nu\to\gamma\nu}$ is performed over occupied orbitals. When the ratio $K_2/((n-1)K_1) = (m-n-1)/4$ is larger than 1, the two-particle transitions dominate and one can neglect the differences in $\overline{\omega}$ and σ for two-particle and one-particle transitions. In this case the spreading width is described by the simple Gaussian form,

$$\Gamma_k(E) \simeq 2\pi(\Delta E)_k^2 \frac{1}{\sigma_k\sqrt{2\pi}} exp\left\{-\frac{(\tilde{E}-E_k-\overline{\omega_k})^2}{2\sigma_k^2}\right\} \tag{47}$$

where $\tilde{E} = E - \delta$. Here $(\Delta E)_k^2$ is the variance defined by Eq.(31) and ω_k and σ_k are close to that for the two-particle transitions. The maximum of $\rho_f(E)$ and $\Gamma(E)$ is shifted by the value $|\overline{\omega_k}|$ towards the center of the spectrum, compared to the maximum of the Breit-Wigner function. This leads to some distortion of the strength function Eq.(33) and the shape of the eigenstates, which is especially large at the bottom of the spectrum.

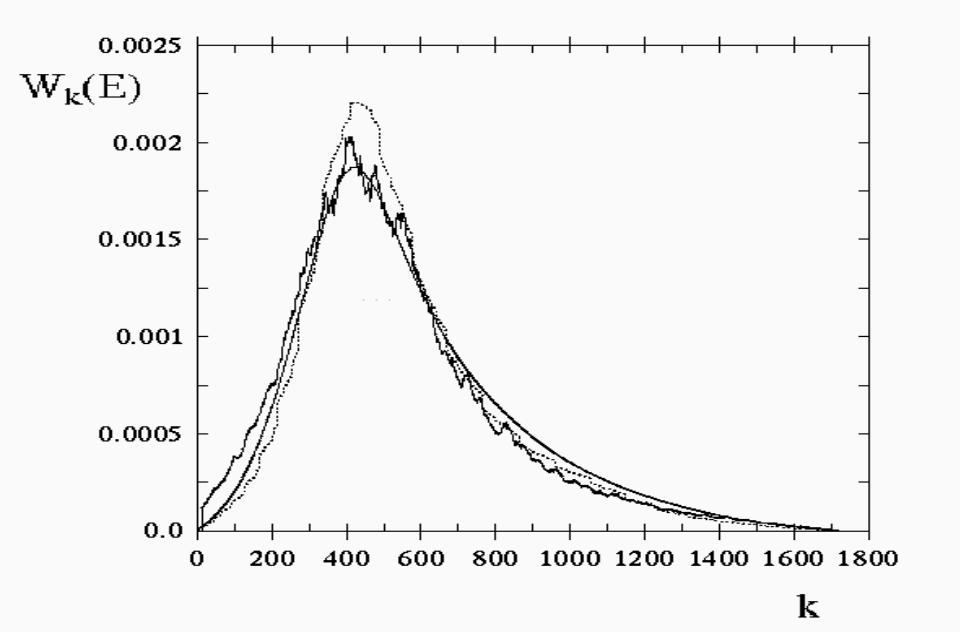

FIG. 10. Shape of the LDOS (33) in the basis representation. Broken line is the result of numerical diagonalization of the TBRI-matrix. To reduce fluctuations, the average over 50 different matrices H_{ik} and over a number of nearby components has been made. The computation has been done for $n = 6$ particles, $m = 13$ orbitals, therefore, the total size of the matrix is $N = 1716$. The interaction strength is $V_0^2 \approx 0.1$ and $d_0 = 1.0$. Dashed and smooth full curves obtained by computation of Eq.(33) with $\Gamma_k(E)$ given by Eqs.(37,38) and by Eq.(47) correspondingly.

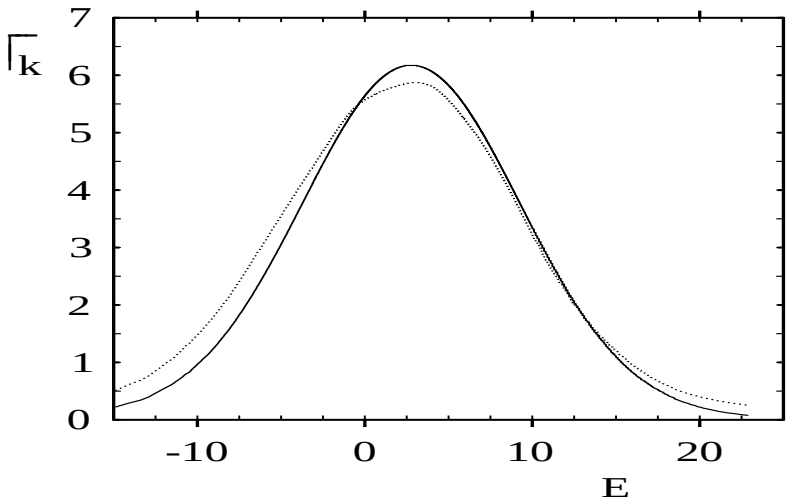

FIG. 11. Dependence $\Gamma_k(E)$ is shown for the parameters of Fig.10. Full curve is the expression (47), the dashed curve is the computation from Eqs.(37, 38).

The above consideration shows that if the interaction is small, $\Gamma \ll \sigma_k$, the strength function has the Breit-Wigner shape with a broad gaussian envelope described by the dependence $\Gamma_k(E)$ in the numerator of Eq. (33). In fact, such a dependence results in the correct (finite) variance of the strength function. When the interaction V increases one needs to take into account one more contribution in Eq.(37) (it was neglected in Eq.(39)). It increases the width of $W_p(E)$ and leads to the estimate $\sigma_k^2 \simeq \sigma_2^2 + \overline{\Gamma_p^2}$. With further increase of interaction, where the shape of $W_p(E)$ is close to the Gaussian, one gets $\sigma_k^2 \simeq \sigma_2^2 + (\Delta E)_k^2$.

Direct numerical study of the model (1) with $n = 6$ Fermi-particles and $m = 13$ orbitals [16] confirmed that the above analytical expressions give quite good description of the shape of the strength function $W_k(E)$ as well as the energy dependence $\Gamma_k(E)$, see Fig.10 and Fig.11. The size of the Hamiltonian matrix is $N = C_m^n = 1716$ and the unperturbed state $i_0 = 440$ was taken.

For the case of quite strong interaction, when $\Gamma \sim \sigma$, the gaussian variation of $\Gamma(E)$ in the numerator of Eq.(33) becomes as important as the variation of the Breit-Wigner energy denominator $(E - E_k)^2 + (\Gamma/2)^2$. In this case the transition from the Breit-Wigner type to Gaussian shape of the LDOS (strength function) takes place. However, still one can use Eqs.(37, 38) and (33) in order to calculate numerically $\Gamma(E), P_k(E)$ and $F(E, E_k)$, taking Γ from Eq.(47) with $\sigma_k^2 \simeq \sigma_2^2 + (\Delta E)_k^2$ as the zero approximation in the right-hand side of Eqs.(37, 38).

F. Non-statistical properties of the TBRI-model

In previous Sections we have considered statistical properties of the TBRI-model based on chaotic structure of the eigenstates and LDOS. However, one should be very careful with this approach since due to underlying correlations in matrix elements of H (see Section 2.1.3), the approach is not always valid, even if all two-body random matrix elements are completely random and independent variables. This fact is due to a two-body nature of interaction and should be taken into account in some cases. Below we show an example when statistical description is incorrect (see details in [13]).

Let us consider a single-particle operator

$$\hat{M} = \sum_{\alpha,\beta} a_\alpha^\dagger \, a_\beta \, M_{\alpha\beta} \; = \sum_{\alpha\,,\beta} \rho_{\alpha\beta} \; M_{\alpha\beta} \tag{48}$$

where $a_\alpha^\dagger$ and a_β are the creation and annihilation operators and we have introduced the density matrix operator $\rho_{\alpha\beta} = a_\alpha^\dagger a_\beta$ which transfers a particle from the orbital β to the orbital α. The matrix element of $\hat{M}$ between compound states can be expressed through the projection of the density matrix into the basis states,

$$\langle n_1 | \, \hat{M} \, | n_2 \rangle = \sum_{\alpha\beta} M_{\alpha\beta} \, \langle n_1 | \, \rho_{\alpha\beta} \, | n_2 \rangle = \sum_{\alpha\beta} M_{\alpha\beta} \, \rho_{\alpha\beta}^{(n_1,n_2)} \tag{49}$$

where

$$\rho_{\alpha\beta}^{(n_1,n_2)} \equiv \sum_{ij} C_i^{(n_1)} \, \langle i | \, \rho_{\alpha\beta} \, | j \rangle \, C_j^{(n_2)} \tag{50}$$

is determined by the exact eigenstates only. In what follows, we are interested in statistical properties of this many-body operator $\hat{\rho}(\alpha, \beta)$ for the fixed orbitals α and β which, on the other hand, determines statistical properties of the single-particle operator $\hat{M}$, see Eq.(48).

One can see that this operator has zero mean,

$$\overline{\rho(\alpha, \beta)} = \overline{\langle n_1 | \, \rho_{\alpha\beta} \, | n_2 \rangle} = 0 \tag{51}$$

if compound eigenstates are truly random.

In general case, the variance of $\hat{\rho}(\alpha, \beta)$ which is of our main interest, has the form,

$$\overline{\rho^2(\alpha, \beta)} = \overline{\langle n_1 | \, \rho_{\alpha\beta} \, | n_2 \rangle \, \langle n_2 | \, \rho_{\beta\alpha} \, | n_1 \rangle} \; =$$

$$\overline{\sum_{i,j,k,l} C_i^{(n_1)} C_j^{(n_1)} C_k^{(n_2)} C_l^{(n_2)} \langle i| \rho_{\alpha\beta} |k\rangle \langle l| \rho_{\beta\alpha} |j\rangle} = S_d^{(n_1,n_2)} + S_c^{(n_1,n_2)} \tag{52}$$

Here we separated the diagonal,

$$S_d^{(n_1 n_2)} = \overline{\sum_{ik} \left|C_i^{(n_1)}\right|^2 \left|C_k^{(n_2)}\right|^2 |\langle i| \rho_{\alpha\beta} |k\rangle|^2} \ , \tag{53}$$

and non-diagonal,

$$S_c^{(n_1,n_2)} = \overline{\sum_{i\neq j,\, k\neq l} C_i^{(n_1)} C_j^{(n_1)} C_k^{(n_2)} C_l^{(n_2)} \langle i| \rho_{\alpha\beta} |k\rangle \langle l| \rho_{\beta\alpha} |j\rangle} \ . \tag{54}$$

contributions to the sum (52) and assumed that eigenstates are real vectors (note that our matrix H_{ij} is symmetric). Typical shape of the density matrix is shown in Fig.12. This shape can be compared with the statistical approach developed in Ref. [46,47] for a very large interaction, in the case when the role of the unperturbed part H_0 is neglected (therefore, the influence of the leading diagonal H_{jj} is small).

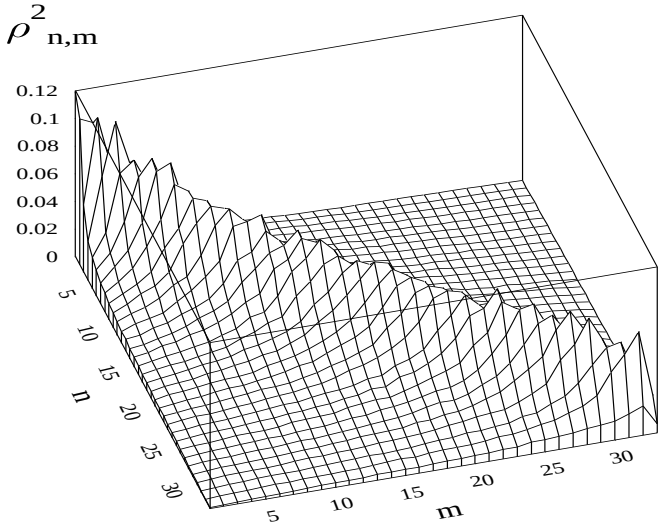

FIG. 12. Form of the density matrix (50) for the TBRI-model with the parameters of Fig.1-5. The quantity $\rho_{n,m} = \left(\overline{\left(\rho_{\alpha\beta}^{(n_1 n_2)}\right)^2}\right)^{1/2}$ is computed with the average inside the blocks of size 10×10 (in the same way as in Fig.2).

As we have discussed in previous Sections, for sufficiently large interaction compound eigenstates $|n\rangle$ of the TBRI-model may be considered as pseudo-random functions due to a very large number of components $C_i^{(n)}$. Therefore, it is natural to expect that the non-diagonal part $S_c^{(n_1,n_2)}$ is zero and the variance is essentially determined by the diagonal term $S_d^{(n_1,n_2)}$ which can be described statistically (for this statistical approach see Refs. [49,19,50]). This assumption has been used in the previous calculations of matrix elements between compound states in [49,19,50,51]. However, recently it was shown [13] that in many-body system these two terms are of the same order, $S_c \sim S_d$, even for completely random two-body interaction. In order to show this very unexpected effect, in Ref. [13] direct computations of the terms S_c and S_d have been performed for the TBRI-model, see Figs.13-14. One can see that the data reveal a systematic difference between the diagonal approximation and exact expression (52). In particular, Fig.14 shows that non-diagonal term S_c is of the same order as S_d which clearly indicates the presence of correlations.

Below, we show how these correlations emerge in the non-diagonal term S_c (for more details see Ref. [13]). First, note that for a given i the sum over k in Eq. (53) for S_d contains only one term, for which $|k\rangle = a_\beta^\dagger a_\alpha |i\rangle \equiv |i'\rangle$, determined by transferring one particle from the orbital α to the orbital β in the state $|i\rangle$ (hereafter we use the notation i' to mark such states). Accordingly, the index i runs over those states in which α is occupied and β is vacant. For such i and i' the matrix element $\langle i| \rho_{\alpha\beta} |i'\rangle = 1$, otherwise, it is zero. Therefore, in fact, the sum in (53) is a single sum, with a number of items less than N,

$$S_d^{(n_1 n_2)} = \overline{\sum_i{}' \left| C_i^{(n_1)} \right|^2 \left| C_{i'}^{(n_2)} \right|^2} \tag{55}$$

where the sum $\sum_i{}'$ runs over the specified i. Analogously, Eq. (54) can be written as the double sum over i and j specified as above,

$$S_c^{(n_1 n_2)} = \overline{\sum_{i \neq j}{}'' C_i^{(n_1)} C_j^{(n_1)} C_{i'}^{(n_2)} C_{j'}^{(n_2)}}, \tag{56}$$

where j' is a function of j, $|j'\rangle = a_\beta^\dagger a_\alpha |j\rangle$. Note that the energies of the basis states and their primed partners are connected as $E_{i'} - E_i = \epsilon_\beta - \epsilon_\alpha = E_{j'} - E_j$.

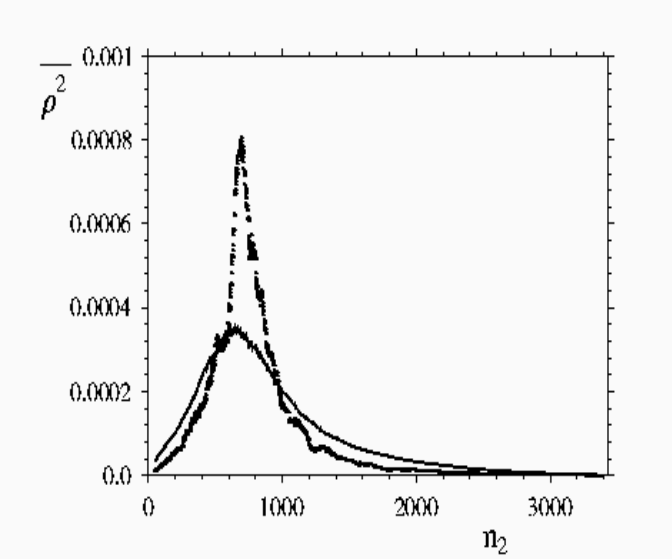

FIG. 13. Mean square matrix element (52) calculated in the TBRI-model for $n = 7$ particles and $m = 14$ orbitals, $\alpha = 7$, $\beta = 8$, as a function of the eigenstate n_2 for $n_1 = 575$ (total size of the matrix is $N = 3432$). Dots correspond to the sum $S_d + S_c$ while the solid line represents the diagonal contribution S_d only [see (53)].

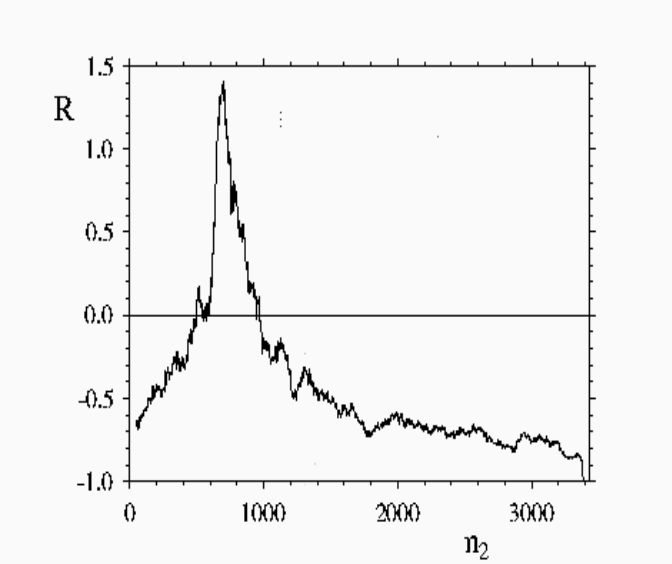

FIG. 14. Ratio $R = S_c/S_d$ of the correlation contribution to the diagonal contribution for the same parameters as in Fig.13.

One can expect that maximal values of the sum (55) and (56) correspond to the terms for which $C-$components are principal components of the eigenstates. This means that mean square of the matrix element $\overline{|\langle n_1|\,\rho_{\alpha\beta}\,|n_2\rangle|^2}$ is maximal when the operator $\rho_{\alpha\beta}$ couples the principal components of the state $|n_1\rangle$ with those of $|n_2\rangle$, i.e. for $E^{(n_1)}-E^{(n_2)}\approx\omega_{\alpha\beta}\equiv\epsilon_\alpha-\epsilon_\beta$. Far from the maximum ($\left|E^{(n_1)}-E^{(n_2)}-\omega_{\alpha\beta}\right|>\Gamma$) a principal component of one state, say, n_1, is coupled to a small component k of the other state n_2 ($\left|E_k-E^{(n_2)}\right|>\Gamma$). The latter case is simpler to consider analytically, since the admixture of a small component in the eigenstate can be found via the standard perturbation theory. This approach reveals the origin of the correlations in the sum S_c, Eq. (56). For example, if $C_j^{(n_1)}$ is a small component of the eigenstate n_1, then it can be expressed as a perturbation theory admixture to the principle components. If the component $C_i^{(n_1)}$ is one of the latter, then there is a term in the sum (56), which is proportional to the principal component squared, $\left|C_i^{(n_1)}\right|^2$.

Based on this consideration, in Ref. [13] was found that far from the maximum, $\left|E^{(n_2)}-E^{(n_1)}-\omega_{\beta\alpha}\right|>\Gamma$, the non-diagonal terms read

$$S_c^{(n_1n_2)}\approx-\frac{2}{\left(E^{(n_2)}-E^{(n_1)}-\omega_{\beta\alpha}\right)^2}\sum_{i,j\prime}{}''\left|C_i^{(1)}\right|^2\left|C_{j'}^{(2)}\right|^2\overline{H_{i'j'}H_{ij}} \tag{57}$$

A similar calculation of the diagonal sum $S_d^{(n_1n_2)}$, Eq. (53), yields

$$S_d^{(n_1n_2)}\approx\frac{1}{\left(E^{(n_2)}-E^{(n_1)}-\omega_{\beta\alpha}\right)^2}$$

$$\times\left\{\sum_i{}'\sum_{j\prime}\left|C_i^{(n_1)}\right|^2\left|C_{j'}^{(n_2)}\right|^2\overline{H_{i'j'}^2}+\sum_i\sum_{j\prime}{}'\left|C_i^{(n_1)}\right|^2\left|C_{j'}^{(n_2)}\right|^2\overline{H_{ij}^2}\right\} \tag{58}$$

Let us estimate the relative magnitudes of S_d and S_c. First, we consider the case when $|i\rangle$ and $|j\rangle$ differ by two orbitals, $|j\rangle=a_{\mu_2}^\dagger a_{\mu_1}a_{\nu_2}^\dagger a_{\nu_1}|i\rangle$, in this case $H_{ij}=V_{\nu_1\mu_1\nu_2\mu_2}$. Since the basis states $|i'\rangle$ and $|j'\rangle$ must differ by the same two orbitals, we have $H_{i'j'}=V_{\nu_1\mu_1\nu_2\mu_2}=H_{ij}$ (note that $\nu_1,\mu_1,\nu_2,\mu_2\neq\alpha,\beta$, since both states $|i\rangle$ and $|j\rangle$ contain α and do not contain β, whereas $|i'\rangle$ and $|j'\rangle$ contain β and do not contain α). Therefore, the averages over the non-zero matrix elements between such pairs of states give $\overline{H_{ij}H_{i'j'}}=\overline{H_{ij}^2}=\overline{H_{i'j'}^2}=V_0^2$.

Now, let us consider the case when $|i\rangle$ and $|j\rangle$ differ by one orbital $|j\rangle=a_{\nu_2}^\dagger a_{\nu_1}|i\rangle$ only. In this case the Hamiltonian matrix elements are sums of the $n-1$ two-body matrix elements, see Eqs.(9) and (10). As was shown in Section 2.1.3, the sums of $n-2$ terms in H_{ij} and $H_{i'j'}$ coincide and the difference is due to the one term only (orbital α is replaced by the orbital β). Thus,

$$\overline{H_{ij}H_{i'j'}}=(n-2)V^2\ ,\qquad\overline{(H_{ij})^2}=\overline{(H_{i'j'})^2}=(n-1)V^2 \tag{59}$$

where we took into account that $\overline{V_{\kappa\lambda\mu\nu}V_{\kappa_1\lambda_1\mu_1\nu_1}}=V^2\delta_{\kappa\kappa_1}\delta_{\lambda\lambda_1}\delta_{\mu\mu_1}\delta_{\nu\nu_1}$.

The contributions of one-particle and two-particle transitions in Eqs. (57) and (58) representing S_c and S_d respectively, are determined by the numbers of such transitions allowed by the corresponding sums. For the single-prime sums in Eq. (58) these numbers are proportional to K_1 and K_2, Eq. (7). In the double-prime sum in Eq. (57) these numbers are proportional to $\tilde{K}_1$ and $\tilde{K}_2$, the numbers of the two-body and one-body transitions $i\to j$, in the situation when one particle and the two orbitals (α and β) do not participate in the transitions. These numbers can be obtained from Eq. (7) if we replace n by $n-1$, and m by $m-2$, so that $\tilde{K}_1=(n-1)(m-n-1)$, $\tilde{K}_2=(n-1)(n-2)(m-n-1)(m-n-2)/4$. Finally one can obtain that for $|E^{(n_2)}-E^{(n_1)}-\omega_{\beta\alpha}|>\Gamma$ the contribution of the correlation term to the variance of the matrix elements of $\rho_{\alpha\beta}$ can be estimated in the ratio as

$$R\equiv\frac{S_c}{S_d}=-\frac{(n-2)\tilde{K}_1+\tilde{K}_2}{(n-1)K_1+K_2}=-\frac{(n-2)(m-n-1)(m-n+2)}{n(m-n)(m-n+3)}. \tag{60}$$

This equation shows that for $n=2$ we have $S_c=0$, which is easy to check directly, since in this case $\overline{H_{i'j'}H_{ij}}=0$. For $n>2$ the correlation contribution S_c is negative in the tails of the LDOS. This means that it indeed suppresses the transition amplitudes off-resonance (see Figs.13-14). For $n,m-n\gg1$ the ratio R approaches its limit value -1. It is easy to obtain from Eq. (60) that for $m-n\gg1$

$$\frac{S_d + S_c}{S_d} = 1 + R \simeq \frac{2m}{n(m-n)} \ . \tag{61}$$

Thus, surprisingly, the role of the correlation contribution increases with the number of particles. This result is supported by numerical data reported in Ref. [13]. In Fig.14 one can see that the suppression of the matrix elements $\overline{\rho^2(\alpha,\beta)}$ due to the correlation term at the tails, is quite strong, numerical ratio is $R \approx -0.7$ vs. $R = -0.55$ obtained from Eq.(60); this should be compared with the case $n = 4, m = 11, N = 330$ for which numerical value is $R \approx -0.45$, see details in [13]. The correlation contribution should be even more important in compound nuclei, where $N \sim 10^5$. This case can be modeled by the parameters $n = 10$, $m = 20$; then we have $R = -0.66$, or, equivalently, $(S_d + S_c)/S_d = 0.34$, which means that the correlations suppress the squared element ρ^2 between compound states by a factor of 3 (far from its maximum).

It is worth emphasizing that the existence of correlations due to the perturbation theory admixtures of small components to the chaotic eigenstates, which leads to a non-zero value of S_c (56), is indeed non-trivial. For example, if one examines the sum of Eq. (56) as a function of i and j, it would be hard to guess that the sum itself is essentially non-zero, since positive and negative values of $\xi_{ij} \equiv C_i^{(n_1)} C_j^{(n_1)} C_{i'}^{(n_2)} C_{j'}^{(n_2)}$ seem to be equally frequent, and have roughly the same magnitude, see Fig.15. However, in spite of apparent random character of the terms ξ_{ij} , its mean value turns out to be non-zero and is of the same order as the diagonal term S_d . Since $\sum_{n_1} S_c^{(n_1 n_2)} = \sum_{n_2} S_c^{(n_1 n_2)} = 0$ (see below), the suppression of $\overline{\rho^2(\alpha,\beta)}$ at the tails should be accompanied by correlational enhancement of the matrix elements near the maximum (for $\left|E^{(2)} - E^{(1)} - \omega_{\beta\alpha}\right| < \Gamma$).

Thus, we come to the important conclusion: even for a random two-body interaction, the correlations produce some sort of a "*correlation resonance*" in the distribution of the squared matrix elements $\overline{\rho^2(\alpha,\beta)}$. One should note that this increase of the correlation effects in the matrix elements of a perturbation can be explained by the increased correlations between the Hamiltonian matrix elements when the number of particles and orbitals increases ($N/n \propto e^n$).

In a similar way one can estimate the size of the correlation contribution S_c near the maximum of the M^2 distribution (at $\left|E^{(n_2)} - E^{(n_1)} - \omega_{\beta\alpha}\right| < \Gamma$) [13].

$$\frac{S_d + S_c}{S_d} = 1 + R_m = 2 - (1 + R_t) \simeq 2\left[1 - \frac{m}{n(m-n)}\right] \ . \tag{62}$$

Comparing the values of the ratio S_c/S_d at the maximum and at the tail in Fig.13 ($n = 7,\ m = 14$) , one can see that indeed, $R_m \approx -R_t$. For larger n and m the correlation enhancement factor asymptotically reaches its maximal value of 2. This numerical example shows the enhancement of $\overline{\rho^2(\alpha,\beta)}$ with respect to S_d at the maximum even greater in size than that predicted by Eq. (62). This is not too surprising since in Eqs. (24)–(62) we estimated the average value of R_m over an interval $\Delta E \simeq \Gamma$ around the maximum rather than the peak value at the maximum.

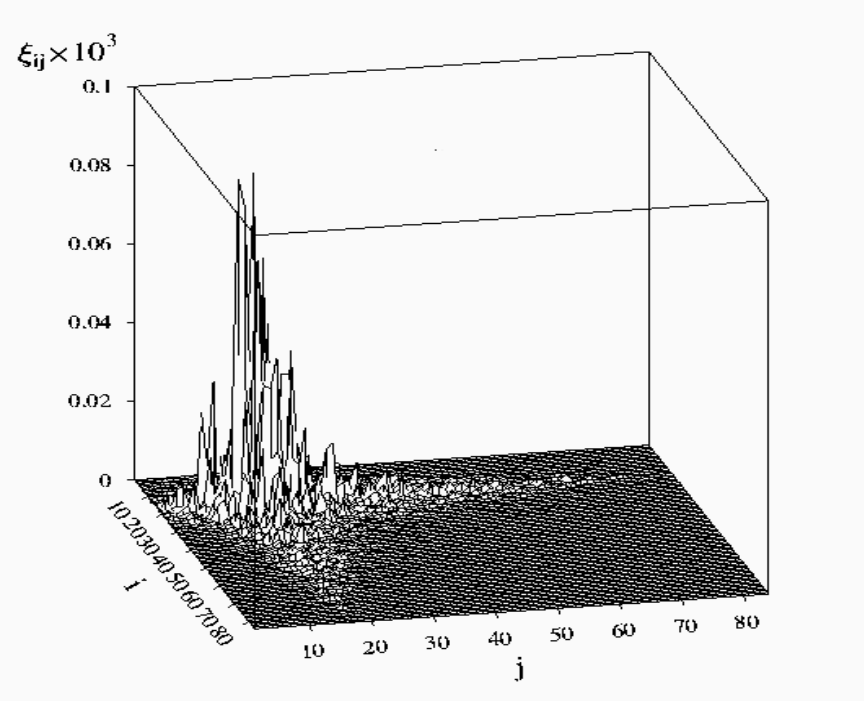

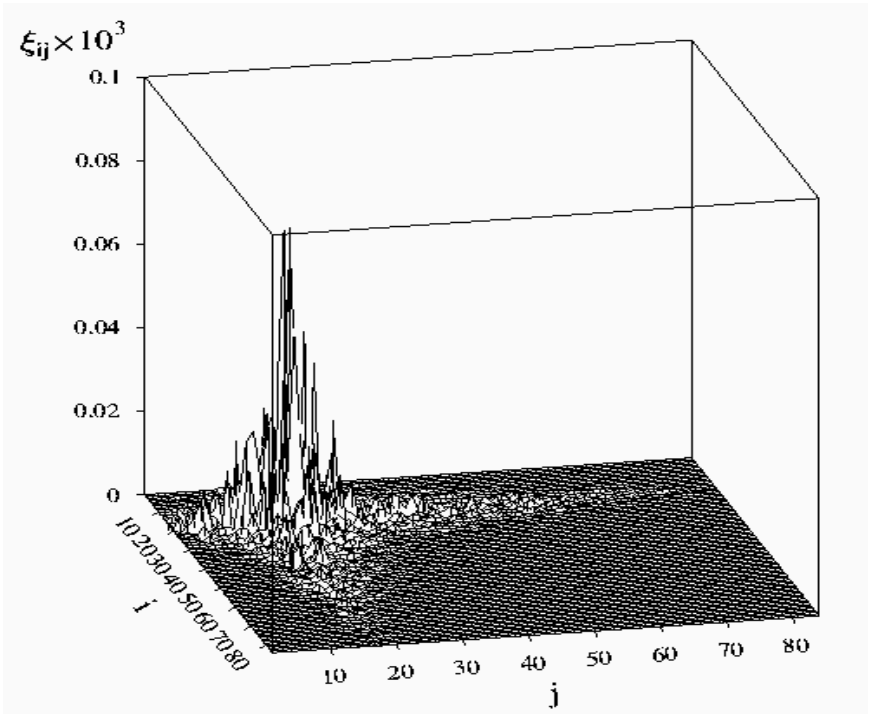

FIG. 15. The distribution of the terms $\xi_{ij} = C_i^{(n_1)} C_j^{(n_1)} C_{i'}^{(n_2)} C_{j'}^{(n_2)}$ of the sum (56) for $n_1 = 55$, $n_2 = 66$, obtained in the TBRI-model for the same set of parameters as in Figs.1-5, averaged over $N_g = 100$ realizations of the interaction. Indices i and j in the figure run over those 84 components in which α is occupied and β is vacant. (a) on the top: positive values, (b) on the bottom: negative values (absolute values).

III. THERMALIZATION AND ONSET OF CHAOS

A. Distribution of occupation numbers

Let us now come back to the distribution of occupation numbers defined by Eq.(5). It gives the probability that one of n particles occupies an orbital s specified by the one-particle state $|s\rangle$, for the fixed exact (compound) state $|i\rangle$. According to this expression, this probability can be found by projecting the state $|i\rangle$ onto the basis of unperturbed states, for which the relation between the positions of all particles in the single-particle basis and specific many-particle basis state is known by the construction of the latter. One can see that the probability $n_s = n_s(E^{(i)})$ is the sum of probabilities over number of basis states which construct the exact state. For Fermi-particles, only one particle can occupy an orbital, this is why the occupation number $n_s^{(k)} = 0$ or 1 .

It is clear that for chaotic eigenstates the n_s-distribution is a fluctuating function of the total energy $E = E^{(i)}$ of a system, due to fluctuations of the components $C_k^{(i)}$ of eigenstates. In order to obtain a smooth dependence, one should make an average over a small energy window centered at $E^{(i)}$, which is in the spirit of conventional statistical mechanics for systems in the contact with the thermostat. In fact, such an average is a kind of microcanonical averaging since it is done for the fixed total energy E of a system. Therefore, in what follows, by the n_s-*distribution* we assume the averaged distribution,

$$n_s(E) = \sum_k \overline{\left|C_k^{(i)}\right|^2} \langle k|\, \hat{n}_s\, |k\rangle = \sum_k F(E_k, E^{(i)}) \text{-} \langle k|\, \hat{n}_s\, |k\rangle \tag{63}$$

where the $F-$function discussed in previous Section is used.

We are going to show that the n_s- distribution plays essential role in the statistical approach to finite systems of interaction particles. Our interest to this quantity is of two-fold. First, the knowledge of the distribution of occupation numbers gives the possibility to calculate mean value of any single particle operator $\langle M\rangle = \sum_s n_s M_{ss}$. Here M_{ss} are diagonal matrix elements of a single-particle operator $\hat{M}$, which very often can be found easily since they refer

single-particle physics. For quantum systems with complex behavior, the non-trivial part is the $F-$function which absorbs the result of the two-body interaction between many basis states. The important point is that in order to find the distribution of occupation numbers, there is no need to know exactly eigenstates of the system. Instead, the shape of eigenstates in the energy representation is needed, which is defined by the $F-$function. Thus, if we know this function and properties of the unperturbed system, one can relate statistical properties of chaotic systems to single-particle quantities.

Moreover, the variance of the distribution of non-diagonal elements of M , describing transition amplitudes between "chaotic" compound states due to a weak external perturbation, can be also expressed through to the occupation numbers n_s . This variance is important from experimental point of view, for example, for the estimate of an enhancement of a weak interaction (which refers, for example, the parity violation in atoms and nuclei) , see details in [51,19,13,21].

Second, the form of the distribution of occupation numbers is interesting itself. One of important questions which arises in this respect, is whether the standard Fermi-Dirac and Bose-Einstein distributions occur for isolated systems of finite number of particle. If they occur, then, under what conditions and how they can be described? One can suggest that the role of the interaction between particles is crucial since this is the only reason to result in a complex behavior (chaos) of a system, and the latter is the mechanism for the statistical equilibrium. Another non-trivial question relates to the meaning of temperature for isolated systems. The study of the n_s-distribution gives a new insight on these and other problems.

For the analytical treatment it is convenient to represent the n_s-distribution in the following form,

$$n_s(E) = \frac{\sum\limits_k n_s^{(k)}\, \tilde{F}(E_k - E\,)}{\sum\limits_k \tilde{F}(E_k - E)} \tag{64}$$

Here the function $\tilde{F}(E_k - E)$ is the part of the $F-$function, which non-trivially depends on the difference $E_k - E$ between the unperturbed energy E_k only. Namely, we omitted the normalization term $f\,(E)$ since the summation in Eq.(64) runs over the unperturbed energy, $F(E_k, E) = f\,(E)\,\tilde{F}(E_k - E\,)$. Thus, the denominator appears due to the normalization. This form (64) allows one to introduce a kind of the *partition function*,

$$Z(E) = \sum_k \tilde{F}(E_k - E) \tag{65}$$

which is entirely determined by the shape of chaotic eigenfunctions.

The above expression (64) gives a possibility of the statistical description of complex systems. Indeed, as was mentioned above, the shape of the $F-$ function has universal features and can be often described analytically. Therefore, in practice there is no need to diagonalize huge Hamiltonian matrix of a many-body system in order to find statistical averages. We would like again to stress that the summation in (64) is carried out over unperturbed energies E_k defined by the mean field, rather than over the energies of exact eigenstates in the standard canonical distribution. As a result, the distribution of occupation numbers can be derived analytically (see below) even for few interacting particles, in a situation when the standard Fermi-Dirac distribution does not occur.

B. Microcanonical vs. canonical distribution

Let us now compare the n_s-distribution (64) with occupation numbers given by the standard *canonical distribution* [15],

$$n_s(T) = \frac{\sum\limits_i n_s^{(i)}\, \exp(-E^{(i)}/T)}{\sum\limits_i \exp(-E^{(i)}/T)} \tag{66}$$

Here T is the temperature of a heat bath and the index i stands for exact eigenstates. The important difference between the n_s- distribution (64) and the canonical distribution (66) is that in Eq. (64) the occupation numbers are calculated for the fixed total energy E of a system unlike the fixed temperature T in Eq.(66). However, both expressions can be compared with each other using the relation between the energy E and the temperature T ,

$$E = \langle E \rangle_T = \frac{\sum\limits_i E^{(i)}\, \exp(-E^{(i)}/T)}{\sum\limits_i \exp(-E^{(i)}/T)} \tag{67}$$

One can show that the canonical distribution corresponds to the average of the "*microcanonical*" n_s- distribution over some energy interval Δ_T . To demonstrate this, let us substitute $n_s^{(i)}$ and $\overline{\left|C_k^{(i)}\right|^2}$ from Eqs.(5,21) into Eq.(66) and replace the summation over i by the integration over $\rho(E^{(i)})\,dE^{(i)}$ where $\rho(E^{(i)})$ is the density of exact energy levels,

$$\sum_i n_s^{(i)} \exp\left(-E^{(i)}/T\right) \approx \int n_s^{(i)} \rho(E^{(i)}) \exp\left(-E^{(i)}/T\right) dE^{(i)} \approx \tag{68}$$

$$\sum_k n_s^{(k)} \int F_k^{(i)}(E_k, E^{(i)}) \rho(E^{(i)}) \exp\left(-E^{(i)}/T\right) dE^{(i)} = \sum_k n_s^{(k)}\, F(T, E_k)$$

Here the function $F(T, E_k)$ is the canonical average of $F_k^{(i)}$,

$$F(T, E_k) = \int F_k^{(i)} \Phi_T(E^{(i)})\, dE^{(i)} \tag{69}$$

with another "canonical (thermal) averaging" function,

$$\Phi_T(E) = \rho(E) \exp\left(-E/T\right) \tag{70}$$

As a result, one can transform the canonical distribution (66) into the form similar to the n_s- distribution (64),

$$n_s(T) = \frac{\sum\limits_k n_s^{(k)}\, F(T, E_k)}{\sum\limits_k F\,(T, E_k)} \tag{71}$$

This distribution can be used for the calculation of the occupation numbers and other mean values in a quantum dot which is in thermal equilibrium with an environment (with no particle exchange).

In many-body systems with large number of particles the function $\Phi_T(E)$ has a very narrow maximum since the density of states $\rho(E^{(i)})$ typically grows very fast. The position E_m of its maximum is defined by the expression

$$\frac{d \ln \rho(E)}{dE} = \frac{1}{T} \tag{72}$$

and the width is given by

$$\Delta_T = \left| \frac{d^2 \ln\, \rho(E)}{dE^2} \right|^{-1/2} \tag{73}$$

Let us consider the TBRI-model (1) for which the density of states is known to be described by the Gaussian,

$$\rho(E) = \frac{1}{\sigma\sqrt{2\pi}} \exp\left(-\frac{(E - E_c)^2}{2\sigma^2}\right) \tag{74}$$

with E_c and σ^2 as the center and the variance of the spectrum. This allows easily to find the form of $\Phi_T(E)$ which also has the gaussian form,

$$\Phi_T(E) = \frac{1}{\sigma\sqrt{2\pi}} \exp\left(-\frac{(E - E_m)^2}{2\sigma^2}\right) \tag{75}$$

with

$$E_m = E_c - \frac{\sigma^2}{T} \tag{76}$$

One can see that the width Δ_T of the thermal averaging function is equal to the gaussian width of the spectrum, $\Delta_T = \sigma$. In Ref. [15] it was argued that for large number of particles both widths Δ_T and ΔE are much smaller than the typical energy interval, $\sigma / |E - E_c| \sim 1/\sqrt{n}$. Therefore, for large number of particles the function Φ_T can be regarded as the delta-function at $E = E_m$ and the n_s- distribution is close to the canonical one, see Eq.(69).

However, the canonical distribution (66) is not correct when describing isolated systems with small number of particles, instead, one should use the n_s- distribution (64), see details below and in [12,15].

C. Transition to the Fermi-Dirac distribution

It is naturally to expect that for a very large number of particles the standard Fermi-Dirac distribution arises from the n_s- distribution (64). Below we reproduce the derivation given in Ref. [15]. By splitting the sum in two parts, which corresponds to the separate summation over $n_s = 0$ and $n_s = 1$, one can represent the expression (64) in the form

$$n_s(E) = \frac{0 + Z_s(n-1, E-\tilde{\epsilon}_s)}{Z_s(n-1, E-\tilde{\epsilon}_s) + Z_s(n, E)} = \frac{1}{1 + \frac{Z_s(n,E)}{Z_s(n-1,E-\tilde{\epsilon}_s)}} \tag{77}$$

where two "partial" partition functions $Z_s(n, E)$ and $Z_s(n-1, E-\tilde{\epsilon}_s)$ are introduced. For the first function the summation is taken over all single-particle states of n particles with the orbital s excluded, $Z_s(n, E) = \sum_k' \tilde{F}(E_k - E)$. Correspondingly, the sum in $Z_s(n-1, E-\tilde{\epsilon}_s)$ is taken over the states of $n-1$ particles with the orbital s excluded. The latter sum results from the terms for which the orbital s is filled ($n_s = 1$) , thus, one should add the energy $\tilde{\epsilon}_s \equiv E_k(n) - E_k(n-1)$ of this orbital to the energy $E_k(n-1)$ of the basis state $|k\rangle$ defined by $n-1$ particles. Since the $F-$ function mainly depends on the difference $E_k + \tilde{\epsilon}_s - E$, the adding term $\tilde{\epsilon}_s$ to $E_k(n-1)$ is the same as its subtraction from the total energy E . Note, that this term is defined by

$$\tilde{\epsilon}_s = \epsilon_s + \sum_{p \neq s} u_{sp} n_p^{(k)} \tag{78}$$

where ϵ_s is the energy of a single-particle state and u_{sp} is the diagonal matrix element of the two-body residual interaction. By taking $\tilde{\epsilon}_s$ independent of k we assume that the averaging over the basis states near the energy E is possible, in fact, this is equivalent to a local (at a given energy) mean field approximation. One should stress that this approximation is important when comparing the simple TBRI-model (1) with realistic systems. For example, for the Ce atom there are orbitals from different open sub-shells (e.g. $4f$ and $6s$) which are quite close in energies, however, they have very different radius. As a result, the Coulomb interaction between the corresponding electrons is very different [52]. In this case the interaction terms in Eq.(78) strongly depend on the occupation numbers of other particles. As a result, the equilibrium distribution for occupation numbers n_s is very different from the Fermi-Dirac distribution [52]. However, the original n_s- distribution (64) for occupation numbers is valid and gives correct result [53]. In other cases like random two-body interaction model [12,13,15] or nuclear shell model [26,28], or the atom of gold [54], such a local mean field approximation is quite accurate and results in the FD-distribution.

For large number $n \gg 1$ of particles distributed over $m \gg 1$ orbitals, the dependence of Z_s on n and $\tilde{\epsilon}_s$ is very strong since the number of terms N in the partition function Z_s is exponentially large, $N = \frac{m!}{(m-n)!n!}$. Therefore, to make the dependence on arguments smooth, one should consider $\ln Z_s$ instead of Z_s . In this case one can obtain

$$\ln Z_s(n - \Delta n, E - \tilde{\epsilon}_s) \approx \ln Z_s(n, E) - \alpha_s \Delta n - \beta_s \tilde{\epsilon}_s \tag{79}$$

$$\alpha_s = \frac{\partial \ln Z_s}{\partial n}; \quad \beta_s = \frac{\partial \ln Z_s}{\partial E}; \quad \Delta n = 1$$

This leads to the distribution of the Fermi-Dirac type,

$$n_s = \frac{1}{1 + \exp(\alpha_s + \beta_s \tilde{\epsilon}_s)} \tag{80}$$

If the number of substantially occupied orbitals in the definition of Z_s is large, the parameters α_s and β_s are not sensitive as to which particular orbital s is excluded from the sum and one can assume $\alpha_s = \alpha \equiv -\mu/T$, $\beta_s = \beta \equiv 1/T$ as in the standard derivation of the Fermi-Dirac distribution for systems in contact with thermostat. Therefore, the chemical potential μ and temperature T can be found from the conditions of fixed number of particles and fixed energy,

$$\sum_s n_s = n; \quad \sum_s \epsilon_s n_s + \sum_{s>p} u_{sp} n_s n_p = \sum_s n_s(\epsilon_s + \tilde{\epsilon}_s)/2 = E \tag{81}$$

Note, that the sums in (81 , 78) containing the residual interaction u_{sp} can be substantially reduced by a proper choice of the mean field basis (for instance, the terms u_{sp} can have different signs in such a basis). In practice, the values ϵ_s and $\tilde{\epsilon}_s$ may be very close. Since in the above expressions (81) the nondiagonal matrix elements of the interaction are

not taken into account, one can expect that the distribution of occupation numbers defined by these equations gives a correct result if the interaction is weak enough (ideal gas approximation). However, below it will be shown that, in fact, even for strong interaction the Fermi-Dirac distribution can be also valid if the total energy E is rescaled in a proper way, by taking into account the increase of the temperature due to statistical effects of the (random) interaction.

One should also note that the above consideration is similar to the standard derivation (see e.g. [42]) of the Fermi-Dirac distribution from the canonical distribution (66) for the case of many non-interacting particles (ideal gas). It is curious that the Fermi–Dirac distribution is very close to the canonical distribution (66) even for very small number of particles, $n \geq 2$, provided the number of essentially occupied orbitals is large (which happens for $T \gg \epsilon$ or $\mu \gg \epsilon$). This fact results from the large number of "principal" terms in the partition function Z_s , and allows one to replace α_s by α in the term $Z_s(n,T)/Z_s(n-1,T) \equiv \exp(\alpha_s + \beta T)$ in the canonical distribution (66) (compare with (77)).

One should stress, however, that the temperature T in the Fermi-Dirac distribution is different from that in the canonical distribution. Indeed, using the expansion $\alpha_s = \alpha(\epsilon_F) + \alpha'(\epsilon_s - \epsilon_F)$ one can obtain the relation between the Fermi-Dirac (β_{FD}) and canonical (β) inverse temperatures, $\beta_{FD} = \beta + \alpha'\epsilon_F$. Concerning the chemical potential, its definition also changes, $-\mu/T = \alpha(\epsilon_F) - \alpha'\epsilon_F$. More specifically, for the same total energy E of the system , the canonical and Fermi-Dirac distributions give the same distribution n_s defined, however, by different temperatures, see details in [12,13,15] and discussion below.

D. Analytical approach to the n_s-distribution

In the previous section it was shown how the standard Fermi-Dirac distribution occurs in the TBRI-model when number of particles is very large. However, the expression (5) for the distribution of occupation numbers via the shape of chaotic eigenstates is of more general form and also valid even when the number of particles is relatively small. In this case the n_s-distribution can be of the form very different from the FD-distribution. Below we show how to analytically derive the n_s-distribution and express it in terms of single-particle and unperturbed many-particle spectrum, using general properties of the $F-$function [15].

For simplicity, we consider the case of relatively strong interaction, when the shape of the LDOS and exact eigenstates can be described by the Gaussian. In order to calculate the occupation numbers n_s, we use the expression (77) containing two partial partition functions $Z_s(n,E)$ and $Z_s(n-1,E-\epsilon_s)$ which correspond to systems with n and $n-1$ particles, with the orbital s is excluded from the set of single-particle states. The partition function can be found from the relation

$$Z(E) = \sum_k \tilde{F}(E_k - E) \approx \int \rho_0(E_k)\tilde{F}(E_k - E)dE_k \tag{82}$$

As was discussed above, the density of unperturbed states $\rho_0(E_k)$ in the TBRI-model it the Gaussian, s

$$\rho_0(E_k) = \frac{N}{\sqrt{2\pi\sigma_0^2}} \exp\left(-\frac{(E_k - E_c)^2}{2\sigma_0^2}\right) \tag{83}$$

where E_c is the center of the energy spectrum and N is the total number of states. If the shape of eigenstates is also described by the Gaussian,

$$\tilde{F}(E_k - E) = \frac{N}{\sqrt{2\pi(\Delta E)^2}} \exp\left(-\frac{(E_k - E)^2}{2(\Delta E)^2}\right) \tag{84}$$

then the integration in (82) can be easily performed. The variance $(\Delta E)^2$ is defined by Eq.(31). It should be pointed out that, strictly speaking, in this expression the center of the $F-$function is shifted by the value $\Delta_1^{(i)}$ from the unperturbed energy, $E = E^{(i)} + \Delta_1^{(i)}$, see details in [15]. This shift is due to the level repulsion which forces eigenvalues $E^{(i)}$ in the lower part of the spectrum to move down. The mean-field energies $E_k = H_{kk}$ do not include the nondiagonal interaction which results in the repulsion. Therefore, the "center " of the $F-$function is shifted by the value $\Delta_1^{(i)} = H_{ii} - E^{(i)}$. This shift is estimated in Ref. [15] as follows,

$$\Delta_1^{(i)} \approx \left(E_c - E^{(i)}\right) \frac{(\Delta E)^2}{2\sigma_0^2} \tag{85}$$

where σ_0^2 is the variance of the unperturbed spectrum. One can see that since the variance $(\Delta E)^2$ of the LDOS is typically much smaller than σ_0^2 , this shift in many cases can be neglected.

Direct integration in Eq.(82) gets

$$Z(E) = \frac{N}{\sqrt{2\pi\sigma^2}} \exp\left(-\frac{(E-E_c)^2}{2\sigma^2}\right) \tag{86}$$

where $\sigma^2 = \sigma_0^2 + (\Delta E)^2$, therefore, the variance of the partition function $Z(E)$ coincides with the variance of the perturbed spectrum. In order to calculate the occupation numbers n_s, one should use the expression (77). Therefore, one needs to find the partition functions $Z_s(n,E)$ and $Z_s(n-1,E-\epsilon_s)$ corresponding to n and $n-1$ particles, with the orbital s excluded from single-particle spectrum. To do this, one needs to calculate the number of states N_s and the center E_{cs} for these truncated systems,

$$N_s(n,m-1) = \frac{(m-1)!}{(m-1-n)!\,n!}; \qquad N_s(n-1,m-1) = \frac{(m-1)!}{(m-n)!\,(n-1)!}$$

$$E_{cs}(n) = \overline{\epsilon_{-s}}\,n\,; \quad E_{cs}(n-1) = (\overline{\epsilon_{-s}})\,(n-1); \quad \overline{\epsilon_{-s}} = \frac{\sum_{p\neq s}\epsilon_p}{m-1} \tag{87}$$

The variance σ_{0s} of the energy distributions can be estimated as

$$\sigma_{0s}^2(n) \approx \sigma_{1s}^2\,n \;\; ; \;\; \sigma_{0s}^2(n-1) \approx (\sigma_{1s}^2)\,(n-1)$$

where σ_{1s}^2 is the variance of single-particle spectrum with the excluded orbital s . Here, for simplicity, we have neglected the Pauli principle which is valid for $m \gg n$. Finally, the distribution of occupation numbers takes the form

$$n_s(E) = \frac{1}{1+R}$$

$$R = \frac{m-n}{n}\frac{\sigma_s(n-1)}{\sigma_s(n)} \exp\left[-\frac{(E-E_{cs}(n))^2}{2\sigma_s^2(n)} + \frac{(E-\epsilon_s-E_{cs}(n-1))^2}{2\sigma_s^2(n-1)}\right] \tag{88}$$

where $\sigma_s^2 = \sigma_{s0}^2 + (\Delta E)^2$. Numerical data for the TBRI-model are presented in Fig.16 from which very good agreement with (88) is seen.

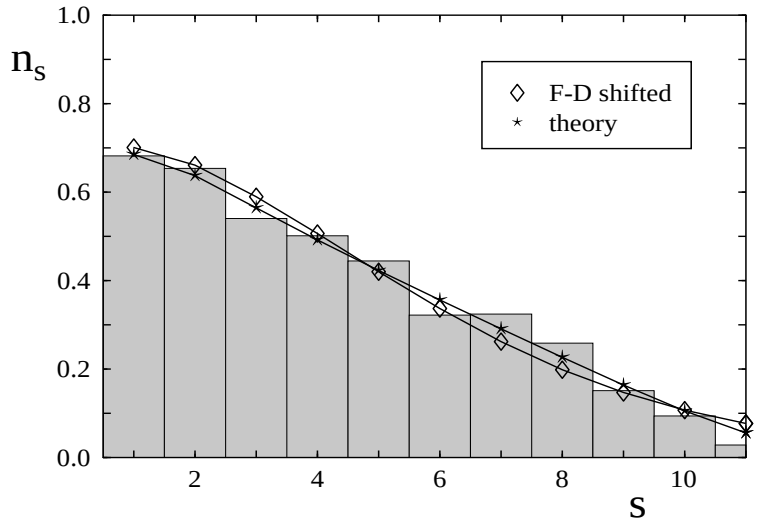

FIG. 16. Analytical description of the occupation numbers. The data are given for the TBRI-model for the parameters of Figs.1-5 ($n=4$, $m=11, V_0=0.12, d_0=1$). The histogram is obtained according to (5) by the averaging over eigenstates with energies taken from a small energy window centered at $E=17.33$ and over 20 Hamiltonian matrices (1) with different realization of the two-body random interaction. Stars represent the analytical expression (88) with σ_{0s} found from the single-particle energy spectrum. Diamonds correspond to the Fermi-Dirac distribution with renormalized energy, see Section 3.5.

It is instructive to compare this result with the Fermi-Dirac distribution which is valid for large number of particles. In this case $R = \exp((\epsilon_s - \mu)/T_{th})$ where $T_{th} = \sigma^2/(E_c - E)$ is the thermodynamic temperature which is discussed below, see (96). The chemical potential μ can be found numerically from the condition of fixed total number of particles n.

E. Effective Fermi-Dirac distribution for finite systems

In previous Section the distribution of occupation numbers has been derived without any reference to the temperature, from the $F-$function and properties of the unperturbed system. However, the n_s-distribution in Fig.16 seems to have a Fermi-Dirac form. One should remind that the latter form in conventional statistical mechanics can be derived for ideal gas of very large *non-interacting* particles. In such a derivation, the presence of the thermostat is assumed, actually, in order to have statistical equilibrium in the system. Indeed, for an isolated systems with large $n \to \infty$, any extremely weak interaction with an environment results in strong statistical properties of a system. Using modern language, one can speak about the *onset of chaos* due to this interaction. In fact, the weakness of the coupling to the heat bath gives the possibility to treat the gas of particles as an ideal gas. It is well known, that in this case one can write the following equations,

$$\sum_s n_s = n, \qquad \sum_s \epsilon_s n_s = E \tag{89}$$

where n and E are total number of particles and total energy, and n_s is assumed to have Fermi-Dirac form,

$$n_s = \frac{1}{1 + \exp(\alpha + \beta\epsilon_s)} \tag{90}$$

When in an isolated system described by the TBRI-model, the number of particles is very large, the above equations result in the FD-distribution, see Section 3.3. However, in such a case the interaction V_0 has to be very weak. Now, if we consider the model with finite and not large number of particles, for a weak interaction there is no chaos in the sense that exact eigenstates have small number of principal components $N_{pc} \ll 1$. Therefore, this model does not allow for its statistical description, in other words, there is no statistical equilibrium. For example, if for such a case we compute the n_s-distribution according to the definition (5), there are very large fluctuations in occupation numbers when slightly changing the total energy $E^{(i)}$, see Fig.17.

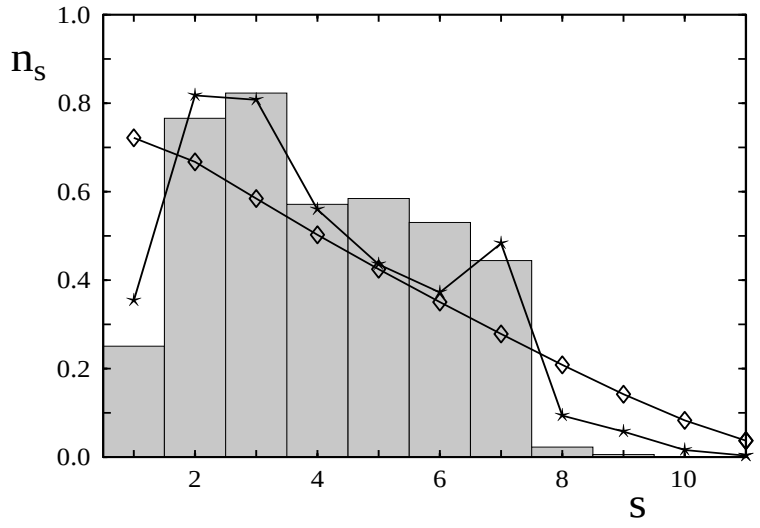

FIG. 17. Absence of a statistical equilibrium for the distribution of the occupation numbers. The histogram is obtained in the same way as in Fig.16, for a very weak interaction $V = 0.02$ which correspond to the region of (II) of the "initial chaotization", see Section 3.7. The total energy is $E^{(i)} = 17.33$. Stars correspond to the theoretical expression (88) which is not valid in this region due to absence of equilibrium. Circles are obtained by direct numerical computation of n_s with the $F-$function taken in a specific form, and with the summation performed over real unperturbed spectrum (instead of the integration with the Gaussian approximation for ρ_o used in Eq. (88)), see details in [15].

In order to have chaotic eigenstates, and, as a result, the possibility of statistical description, one needs to increase the interaction in order to exceed the threshold $V_0 \geq d_f$ (see also discussion in Section 3.7). The less number of particles, the stronger interaction is needed since the two-particle density $\rho_f = d_f^{-1}$ strongly depends on the number of particles. On the other hand, if interaction is strong, the second equation in Eq.(89) is not correct and can not be used for the derivation of the n_s-distribution. To demonstrate this, in Ref. [15] the distribution of occupation numbers n_s for the two-body random interaction model has been directly computed according to Eq.(5) from exact eigenstates of the Hamiltonian matrix (1), see also [12,15]. These data for the "experimental" values of n_s are shown in Fig.18 by the histogram which is obtained from the average over small energy window in order to smooth the fluctuations (with additional averaging over different realizations of the two-body random matrix elements). To compare with the standard Fermi-Dirac distribution, Eqs.(89) have been also numerically solved in order to find the temperature and chemical potential, the resulting n_s-distribution is shown by circles. One should stress that the value of the energy E in (81) was taken the same as for the exact eigenstates from which actual distribution of n_s was computed, namely, $E \approx E^{(i)}$. The comparison of the actual distribution (histogram) with the "theoretical " one, reveals a big difference for a chosen (quite strong) perturbation $V = 0.20$.

To describe correctly the n_s-distribution in terms of the Fermi-Dirac distribution, in Ref. [15] it was suggested to renormalize the total energy of the systems due to the interaction between particles, and instead of Eq.(89) to solve the following equations,

$$\sum_s n_s = n, \qquad \sum_s \epsilon_s n_s = E + \Delta_E \tag{91}$$

where Δ_E is the shift of the total energy due to the interaction. In Ref. [15] it was argued that in the case of random interaction, this term absorbs statistical increase of the energy and gives the correct result for the n_s-distribution. In fact, this assumption is based on a deep equivalence between the *external chaos* originated by the heat bath in the case of open systems, and *internal chaos* due to a random character of the interaction. Therefore, it was assumed that random interaction and chaos in closed systems plays the role of a heat bath.

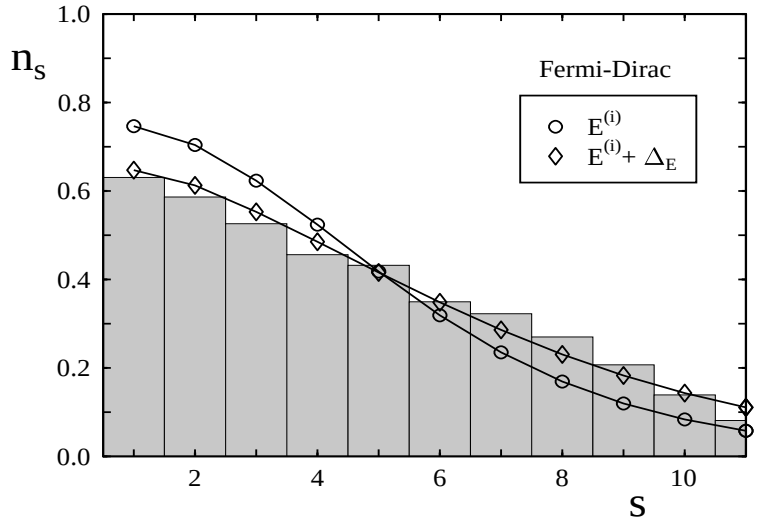

FIG. 18. Fermi-Dirac distribution with and without additional shift of energy due to a (strong) interaction, $V_0 = 0.20$ (other parameters are the same as in Fig.16). Circles stand for the Fermi-Dirac distribution obtained for the total energy $E = 17.3$ corresponding to the energy of eigenstates, see (81). Diamonds correspond to the distribution obtained for the energy shifted according to Eq. (93).

In order to find analytically the shift Δ_E , one needs to consider the structure of exact eigenstates in the unperturbed basis, in particular, to find the shift between the energy of an exact eigenstates and the mean energy of the components of the same eigenstate [15]. Since the density of states rapidly increases with the energy E , the number of higher basis states admixed to an eigenstate due to the interaction is larger than the number of lower basis states. As a result, the mean energy

$$\langle E_k \rangle_i = \sum_k E_k F_k^{(i)} \approx \int E_k F_k^{(i)} \rho_0(E_k) dE_k \tag{92}$$

of the components in an exact eigenstate $|i\rangle$ is higher than the eigenvalue $E^{(i)}$ corresponding to this eigenstate (we consider here the eigenstates in the lower part of the spectrum). There is another effect which decreases the value of $\langle E_k \rangle_i$, see (92), which remains even if the density of states does not depend on the energy. This second effect is due to repulsion between energy levels, according to which the eigenvalues move down for this part of the spectrum, therefore, the difference between $\langle E_k \rangle_i$ and $E^{(i)}$ increases due to the interaction. The second effect also shifts the "center" of the $F-$function. One should stress that all effects leading to the above shift of the energy are automatically taken into account in the relation (92). Thus, one can analytically calculate this shift $\Delta_E = \langle E_k \rangle_i - E^{(i)}$ from the equation (92). For this, one needs to know the unperturbed density of states and the form of $F-$function. The evaluation of the shift Δ_E has been done in [15] by assuming some generic form for the $F-$ function which is valid in a wide range of the interaction strength V ,

$$\Delta_E = \langle E_k \rangle_i - E^{(i)} = \frac{(\Delta E)^2}{\sigma_0^2} (E_c - E) \tag{93}$$

where E_c is the center of the energy spectrum.

Thus, to find correct values for the occupation numbers in the Fermi-Dirac distribution, we should solve Eqs.(91) with Δ_E defined by Eq.(93). The resulting n_s-dependence is shown in Fig.18 by diamonds. As one can see, such a correction gives quite good correspondence to the numerical data. Similar difference occurs for larger number of particle (and smaller interaction strength), see Fig.19 where due to serious numerical problems, the data for the occupation number distribution are given without direct comparison with actual n_s-distribution.

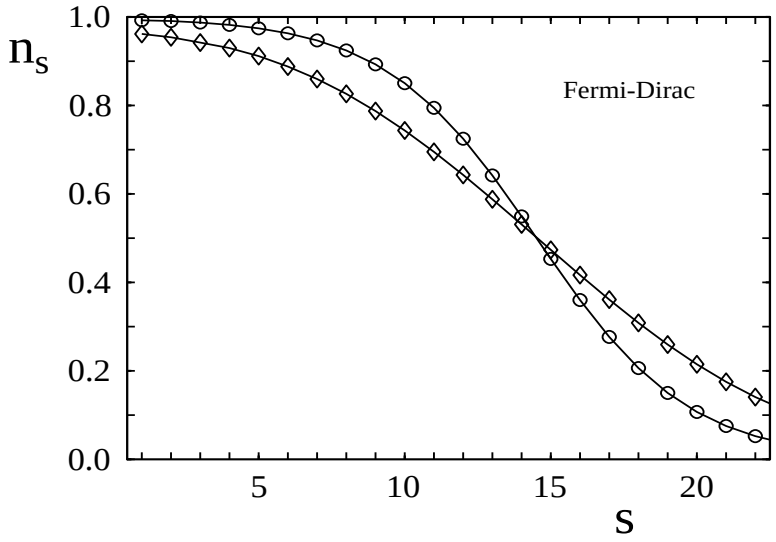

FIG. 19. The same as in Fig.18 for large number of particles, $n = 14$, and orbitals, $m = 28$, for $V_0 = 3 \cdot 10^{-3}$ and $d_0 = 1$. The histogram is not possible to obtain numerically in the direct computation, due to a very large size of the Hamiltonian matrix, $N = 330000$.

To check the analytical prediction (93) for the shift Δ_E , this shift has been directly calculated by comparing the energy $E^{(i)}$ of exact eigenstates with the energy $\langle E_k \rangle_i$. The latter has been numerically found from the exact relation $\langle E_k \rangle_i = \sum_k E_k \left| C_k^{(i)} \right|^2$ (compare with (92)). The comparison of these data (circles in Fig.20) with Eq. (93) (straight full line) shows reasonable agreement, if to neglect strong fluctuations around the global dependence. These fluctuations are due to fluctuations in the components of specific exact eigenstates $|i\rangle$ (note, that the presented data correspond to individual eigenstates, without any additional averaging).

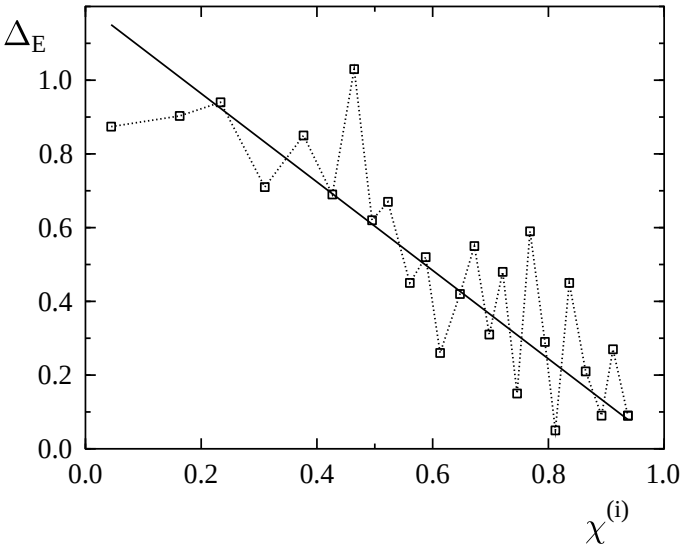

FIG. 20. Shift of the total energy for the corrected Fermi-Dirac distribution. The data are given for the TBRI-model with $n = 4, m = 11, d_0 = 1, V = 0.12$. The straight line is the analytical expression (93), the dotted line (squares) presents direct computation of the shift based on the diagonalization of the Hamiltonian (1) with the following computation of the $< E_k >_i$. On the horizontal axes the rescaled energy $\chi^{(i)} = (E^{(i)} - E_{fermi})/(E_c - E_{fermi})$ is plotted.

F. Temperature vs. chaos

In previous Section it was shown that if the n_s-distribution for finite number of particles in the TBRI-model has the from of the Fermi-Dirac distribution, it can be found from the modified Eq.(91). These equations also determine the parameters α and $T = \beta^{-1}$ which may be associated with the "*chemical potential*" and "*temperature*" for an isolated system. One can see, that due to the shift Δ_E of the total energy in Eq.(91), there is a corresponding shift of the temperature ΔT . It is important to note that in systems with infinite number of particles, all definitions of temperature give the same result. In contrast to this, for finite number of particles different definitions give different results.

Let us, first, start with the standard definition of temperature,

$$\frac{1}{T_{th}} = \frac{dS_{th}}{dE} = \frac{d \ln \rho}{dE} \tag{94}$$

where S_{th} is the thermodynamical entropy,

$$S_{th} = \ln \rho(E) + const \tag{95}$$

and $\rho(E)$ is the density of states.

In fact, this definition of the *thermodynamical temperature* stems from the estimate of the position of maximum of the canonical averaging function $\Phi_T(E)$, see (70), if we assume that the position of its maximum E_m coincides with the energy E of a system. One should stress that in the above definition $\rho(E)$ is the total density of states, therefore, the interaction is essentially taken into account.

Another definition, which is consistent with the first law of thermodynamics (energy conservation), is given by the relation $\langle E \rangle_T = E$, see Eq.(67). Here the averaging is performed over the canonical distribution (66). Since the width Δ_T of the canonical averaging function $\Phi_T(E)$ is not zero, the two definitions of the temperature, (94) and (67)

give, in principal, different values. Indeed, in the case of the Gaussian form of $\rho(E)$ the value of T_{th} given by (94) takes the form (see also [26,28]),

$$T_{th} = \frac{\sigma^2}{E_c - E} \tag{96}$$

where E_c and σ are the center and the width of the total density $\rho(E)$.

On the other hand, direct evaluation of the relation (67) leads to the following definition of the *canonical temperature*,

$$T_{can} = \frac{\sigma^2}{E_c - E + \Delta} \tag{97}$$

Here, the shift Δ is approximately given by the expression

$$\Delta = \frac{\sigma}{K}\left[\exp\left(-\frac{(E_{\min} - E_m)^2}{2\sigma^2}\right) - \exp\left(-\frac{(E_{\max} - E_m)^2}{2\sigma^2}\right)\right] \tag{98}$$

where

$$K = \int_{x_{\min}}^{x_{\max}} \exp\left(-\frac{x^2}{2}\right) dx \approx \sqrt{2\pi} \;\; ; \;\; x = \frac{E - E_m}{\sigma} \;\; ; \;\; E_m = E_c - \frac{\sigma^2}{T_{can}} \tag{99}$$

One can see that the shift Δ itself depends on the temperature, it is proportional to the width $\Delta_T = \sigma$ of the function $\Phi_T(E)$. In the above expressions, $E_{\min}$ and $E_{\max}$ are the low and upper edges of the energy spectrum. Note that the relation $\Delta = 0$ occurs at the center of the spectrum, therefore, at the center the temperature diverges and in the upper part of the spectrum is negative. This fact is typical for systems with bounded spectrum, for example, for spin systems. In fact, the TBRI-model (1) with finite number m of orbitals can be treated as a model for one open shell in atoms, nuclei, clusters, etc. However, in realistic many-body systems there are always higher shells which contribute to the density of states for higher energy. Thus, the density of states $\rho(E)$ is a monotonic function which results in the positive temperature. For such physical applications, the model (1) with finite number of orbitals is reasonable in the lower part of the energy spectrum where the influence of higher shells can be neglected.

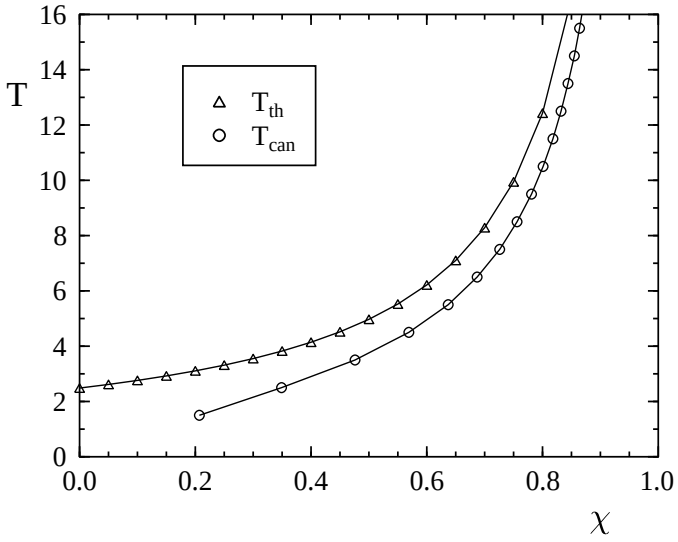

FIG. 21. Different temperatures versus the rescaled energy $\chi = (E - E_{fermi})/(E_c - E_{fermi})$ for the TBRI-model . Parameters are the same as in Fig.16. Triangles stand for the thermodynamical temperature T_{th} defined by (96) and should be compared to the canonical temperature T_{can} (circles), see (97). The width σ of the perturbed density of states is defined by the residual interaction $V_0 = 0.12$ according to (31) and the relation $\sigma^2 = \sigma_0^2 + (\Delta E)^2$ with σ_0 found numerically from the unperturbed many-particle energy spectrum.

One can also see that the difference between the two equations of state $T(E)$ defined by Eqs.(96) and (97), disappears for highly excited eigenstates (for which $E_m - E_{\min} \gg \sigma$), or in large systems with $n \gg 1$. Indeed, one can obtain, $E_c - E \sim n\sigma_1$, where σ_1 is the width of single-particle spectrum. On the other hand, according to the central limit theorem, the variance of total energy spectrum can be estimated as $\sigma_0^2 = \sum_n \sigma_1^2 \approx n\sigma_1^2$, therefore, the ratio $\sigma/(E_c - E) \sim 1/\sqrt{n}$ tends to zero at $n \to \infty$. As was mentioned above, in such realistic finite systems like atoms and nuclei, the number of particles in an open shell is relatively small ($n = 4$ for the Ce atom [19] and $n = 12$ in nuclear shell model [26,28]), therefore, the corrections to the thermodynamical temperature (94) may be important, especially, for low energies. The detailed discussion of different temperatures in nuclear shell model is given in [26,28].

The energy dependence of temperatures T_{th} and T_{can} , as well as the temperature $T_{\exp}$ found directly from the numerical simulation, is shown in Fig.21. The data refer the TBRI-model with $n = 4$ interacting Fermi–particles and $m = 11$ orbitals. The comparison of the thermodynamical temperature T_{th} defined by (96), with the "canonical" temperature (97) reveals quite strong difference in all the range of the rescaled energy $\chi = (E - E_{fermi})/(E_c - E_{fermi})$.

Now let us find the shift of the temperature ΔT which is due to the interaction, see previous Section. Since it is directly related to the shift of total energy, $E \equiv \langle E_k \rangle_i = E^{(i)} + \Delta_E$, one can get,

$$T = T_0 + \Delta T = \frac{\sigma_0^2}{E_c - E^{(i)} - \Delta_E} \approx \frac{\sigma_0^2}{E_c - E^{(i)}} + \frac{(\Delta E)^2}{E_c - E^{(i)}} \tag{100}$$

Therefore, statistical effects of random interaction can be directly related to the increase of temperature of a system, $\Delta T/T_0 = (\Delta E)^2/\sigma_0^2$.

One of the important questions deals with thermodynamical description of isolated systems of interacting particles. In any thermodynamical approach one needs to define, in a consistent way, such quantities as entropy, temperature and equation of state. This problem has been recently discussed [26,28] in application to shell models of heavy nuclei. In particular, it was shown that for a realistic residual interaction different definitions of temperatures give the same result.

G. Transition to chaos and statistical equilibrium

Let us now summarize the discussed above results for the TBRI-model in what concerns transition to chaos and thermalization. The latter term is not defined for isolated systems, our suggestion is to treat "*thermalization*" as the onset of *statistical equilibrium*. The latter allows to give a reasonable statistical description and may be used to find thermodynamical description.

Depending on the strength of (two-body) interaction between particles , one can fix different situations in the model. First region (I) refers *strong (perturbative) localization*. This occurs when the interaction is very weak, $V_0 \ll d_f$ and standard perturbation theory gives correct result. In this case exact eigenstates have only few relatively large components ($N_{pc} \sim 1$) , in other words, the eigenstates are strongly localized in the unperturbed basis. This situation is quite typical for lowest eigenstates (where the density of states is small) even if for higher energies the eigenstates can be considered as very "chaotic" ones ($N_{pc} \gg 1$) .

The second region (II) is characterized by an *initial chaotization* of exact eigenstates which corresponds to a relatively large, $N_{pc} \gg 1$ number of principal components and $V < d_f$. The latter condition is essential since it results in very strong (non-Gaussian) fluctuations of components $C_k^{(i)}$ [55] for the fixed energy $E^{(i)}$ of compound state $|i\rangle$. Such a type of fluctuations reflects itself in a specific character of eigenstates, namely, they turn out to be *sparsed*. As a result, the number of principal components can not be estimates as $N_{pc} \approx \Gamma/D$, as is typically assumed in the literature. In this case the energy width Γ of both the LDOS and eigenstates can be approximately describe as $\Gamma \approx 2\pi V_0^2/d_f$. In Fig.17 it is shown how the distribution of occupation numbers n_s looks like for the TBRI-model (1) with $n = 4$ particles and $m = 11$ orbitals and very weak perturbation $V/d_0 \approx 0.02$. One can see that the distribution of occupation numbers has nothing to do with the Fermi-Dirac distribution (full diamonds), it turns out to be even the non-monotonic function of the energy ϵ_s of orbitals (see also [12]). Note that the averaging procedure used in Fig.17 can not wash out strong fluctuations in occupation numbers n_s .

With further increase of the interaction, where $N_{pc} \gg 1$ and $V > d_f$, the region (III) of the *statistical equilibrium* emerges. In this region the fluctuations of eigenstate components $C_k^{(i)}$ are of the Gaussian form [55] and one can introduce the $F-$function (64) as the shape of exact eigenstates in the unperturbed energy basis. Correspondingly, the fluctuations of the occupations numbers n_s are small in accordance with the central limit theorem, $\Delta n_s/n_s \sim N_{pc}^{-1/2} \ll 1$ for $n_s \sim 1$. One should stress that in this region the value of N_{pc} is given by the common estimate, $N_{pc} \sim \Gamma/D$. As a result, the n_s-distribution changes slightly when changing the energy of a system. Such a situation can be naturally related to the *onset of thermal equilibrium*, though the form of the distribution n_s can be

quite different from the Fermi-Dirac distribution. In this case, the $F-$distribution allows for a correct description of an actual distribution of occupation numbers in isolated quantum systems of interacting particles. One can see that the equilibrium distribution for the occupation numbers arises for much weaker condition compared to that needed for the Fermi-Dirac distribution. Since the energy interval d_f between directly coupled basis states is small, it is enough to have a relatively weak residual interaction $V > d_f$ in order to have the equilibrium distribution (note, that the value of d_f decreases rapidly with the excitation energy).

Next region (IV) is where the *canonical distribution* (66) occurs; for this case in addition to the equilibrium, one needs to have large number of particles, $n \gg 1$. If, also, the condition $\Gamma \ll nd_0$ is fulfilled, the standard Fermi-Dirac distribution is valid with a proper shift of the total energy due to the interaction, see Section 3.5. Typically, this region is associated with the onset of the canonical thermalization (see, for example, [26,28]). In practice, the condition (IV) of the canonical thermalization is not easy to satisfy in realistic systems like atoms or nuclei since n in the above estimates is, in fact, the number of "active" particles (number of particles in a valence shell) rather than the total number of particles. Thus, the description based on the $F-$distribution (64) which does not require the canonical thermalization condition (IV), is more accurate.

The above statements are confirmed by the direct numerical study of the two-body random interaction model [12,15] with few particles when changing the interaction strength V/d_0. If, instead, we increase the number of particles keeping the interaction small, $V \ll d_0$, the distribution (64) tends to the Fermi-Dirac one as it is expected for the ideal gas, see [15].

IV. CONCLUDING REMARKS

In this paper we have discussed a novel approach to isolated systems of finite number of interacting particles. The goal of this approach is a direct relation between the average shape of exact eigenstates ($F-$function), and the distribution n_s of occupation numbers of single-particle levels. From this relation one can see that there is no need to know exactly the eigenstates, instead, if these eigenstates are chaotic (random superposition of a very large number of components of basis states), the $F-$function absorbs statistical effects of interaction between particles and determines the form of the n_s-distribution. Therefore, the structure of chaotic eigenstates in dependence on the model parameters, is the central question in this approach.

The results discussed above relate to the TBRI-model for which all two-body matrix elements are assumed to be random and independent variables. This assumption was made in order to study limiting statistical properties of this model. In particular, it was shown that even in this limit case of completely random (two-body) interaction, the Hamiltonian matrix in many-particle representation can not be treated as the random matrix, therefore, the RMT is, strictly speaking, not valid. However, under some conditions exact eigenstates turn out to be quite random and statistical approach is correct, however, one should take into account the form of eigenstates in a given basis of unperturbed part H_0 .

Another reason for the study of this TBRI-model, is that it is very convenient for the demonstration of the developed approach. In this case there are no any effects of regular motion in the system, and many of analytical estimates can be obtained in a clear way. In particular, it was shown how to calculate the n_s- distribution from the shape of eigenstates, provided the unperturbed spectrum of energy is known. One can stress that in this way one can analytically obtain the n_s-distribution which can have the form very different from the standard Fermi-Dirac distribution. On the other hand, for sufficiently large interaction the n_s-distribution is of the Fermi-Dirac form, therefore, it is convenient to introduce an effective "temperature " and "chemical potential " which give correct description of actual n_s-distribution in terms of the Fermi-Dirac distribution. To do this, one needs to find the shift of the total energy which formally comes into equations determining the FD-distribution. One should stress that this shift is directly related to the $F-$function and can be found analytically.

Now, we would like to point out that the approach discussed in this paper for the TBRI-model is of generic and can be applied both for random and dynamical interaction. One of the most interesting problems is the application of the approach to dynamical systems with the well-defined classical limit. In this situation exact eigenstates in the corresponding quantum model can be expected to appear when two conditions are fulfilled. The first one is the strong chaos in the classical counterpart, and the second is the semi-classical limit (which is typically equivalent to a high energy of a system). Under these two conditions, eigenstates of quantum model have many components and these components may be treated as pseudo-random, thus leading to a statistical equilibrium in the system and possibility to apply the suggested approach.

In Refs. [40,18,17] two quantum dynamical systems have been studied and compared to their classical limits. In both cases the main results refer the region of parameters where the classical motion is strongly chaotic. One of the important questions which was under close investigation is the quantum-classical correspondence for the $F-$function

and the LDOS. As was pointed out in Ref. [39], there is a quite clear and easy way for finding *classical $F-$function* and *classical LDOS*. It is instructive to explain this approach since it is of generic and can be used in many physical applications (see details in [40,18,17]).

Let us start with the classical $F-$function. We assume that the total Hamiltonian can be represented in the form,

$$H = H_0 + V \; ; \quad H_0 = \sum_{k=1}^{n} H_k^0 \; ; \quad H_k^0 = H^0(p_k, x_k) \tag{101}$$

Here H_0 stands for the "unperturbed " Hamiltonian which is the sum of partial Hamiltonians H_k describing the motion of different (non-interacting) n particles. The interaction between particles is embedded in V which is assumed to result in chaotic behavior of the (total) system. Note that the same consideration is valid if instead of particles we mean different degrees of freedom for one particle. Now let us fix the total energy E of the Hamiltonian $H(t)$ and find (numerically) the trajectory $p_k(t)$, $x_k(t)$ by computing Hamiltonian equations. Since the total Hamiltonian is chaotic, there is no problem with the choice of initial conditions $p_k(0)$, $x_k(0)$, any choice gives the same result if one computes for sufficiently large time. When time is running, let us collect the values of *unperturbed* Hamiltonian $H_0(t)$ for fixed values $t = T, 2T, 3T, \ldots$, and construct the distribution of energies $E_0(t)$ along the (chaotic) trajectory of the *total* Hamiltonian H . In such a way, one can get some distribution $W(E_0; E = const)$. Comparing with the quantum model, one can see that this function $W(E_0; E = const)$ is the classical analog of the $F-$function which is the average shape of eigenstates in energy representation. Indeed , any of exact eigenstates corresponds to a fixed total energy $E = const$ and it is represented in the unperturbed basis of H_0 , in fact, $F-$function is the (average) projection of exact eigenstate onto the set of unperturbed ones. Thus, one can expect that for chaotic eigenstates in a deep semiclassical region the two above quantities, classical and quantum ones, correspond to each other.

On the other hand, one can consider the complimentary situation. Let us fix the *unperturbed* energy E_0 and compute a trajectory $p_k^{(0)}(t)$, $x_k^{(0)}(t)$ which belongs to the unperturbed Hamiltonian $H_0(t)$. Similar to the previous case, let us put this unperturbed trajectory into the total Hamiltonian $H(t)$ and collect the values of total energy $E(t)$ along the unperturbed trajectory for discrete values of time. In this way one can find the distribution $\tilde{W}(E; E_0 = const)$ which now should be compared with the LDOS in the corresponding quantum model. However, in this case one should be careful and make an average over many initial conditions $p_k(0)$, $x_k(0)$ with the same energy E_0 , if the unperturbed Hamiltonian is regular. In fact, the above two classical distributions $W(E_0; E = const)$ and $\tilde{W}(E; E_0 = const)$ determine the ergodic measure of energy shells, the first one, when projecting the phase space surface of H onto H_0 , and in the second one, the surface of H_0 onto H (see discussion in [39]).

Numerical data for two different dynamical models have shown amazingly good correspondence between the $F-$function and the LDOS, and their classical counterparts, see details in Refs. [40,18,17]. Recently, few other systems have been studied both in classical and quantum representations, and again, very good correspondence has been numerically found in the semiclassical region. These data confirm the theoretical predictions, and seems to be very important in view of future developments of the semiclassical theory of dynamical chaotic systems. It is important to point out that the above correspondence opens a new way for the *semi-quantal* description of quantum system, when the form of the $F-$function is taken from a classical model and used in order to find distribution of occupation numbers n_s of single-particle levels in the corresponding quantum system [56].

Another interesting problem which has been studied in dynamical systems, is the distribution of occupation numbers and the possibility of its analytical description in the same way as it was done for the TBRI-model (see details in [17]). One of the most interesting results obtained numerically, is that the canonical distribution occurs in an isolated (dynamical) system of only two interacting spin-particles, if one randomize the *non-zero elements* of the interaction V as close as possible to the dynamical constrains of the model. This means that random interaction indeed plays a role of the heat bath and allows to use statistical and thermodynamical description for isolated systems.

V. ACKNOWLEDGMENTS

I am very grateful to my co-authors F.Borgonovi, G.Casati, B.V.Chirikov, V.V.Flambaum, Y.Fyodorov, G.F.Gribakin and I.Guarneri, with whom the works have been done on the subject discussed in this review. This work was supported by CONACyT (Mexico) Grant No. 28626-E.

[1] C.E. Porter, *Statistical Theory of Spectra: Fluctuations* (Academic Press, New York, 1965).
[2] M.L. Mehta, *Random Matrices* (Academic Press, New York, 1967).
[3] T.A. Brody, J. Flores, J.B. French, P.A. Mello, A. Pandey, and S.S.M. Wong, *Rev. Mod. Phys.*, **53** (1981) 385.
[4] T. Guhr, A. Müller-Groeling, and H.A. Weidenmüller, *Phys. Rep.*, **200** (1999) 189.
[5] I.I. Gurevich, *Zh. Eksp. Teor. Fiz.*, **9** (1939) 1283.
[6] O. Bohigas and M.-J. Giannoni, *Lect. Notes Phys.*, **209** (1984) 1.
[7] F.M. Izrailev, *Phys. Rep.*, **196** (1990) 299.
[8] Y.F. Fyodorov and A.D. Mirlin, *Int. J. Mod. Phys.*, **8** (1994) 3795.
[9] E.P. Wigner, *Ann. Math.*, **62** (1955) 548; *Ann. Math.*, **65** (1957) 203.
[10] J. B. French and S. S. M. Wong, *Phys. Lett. B*, **35** (1970) 5.
[11] O. Bohigas and J. Flores, *Phys. Lett. B*, **34** (1971) 261.
[12] V.V. Flambaum, F.M. Izrailev, and G. Casati, *Phys. Rev. E*, **54** (1996) 2136.
[13] V.V. Flambaum, G.F. Gribakin and F.M. Izrailev, *Phys. Rev. E*, **53** (1996) 5729.
[14] V.V. Flambaum and F.M. Izrailev, *Phys. Rev. E*, **55** (1997) R13.
[15] V.V. Flambaum and F.M. Izrailev, *Phys. Rev. E*, **56** (1997) 5144.
[16] V.V. Flambaum and F.M. Izrailev, Phys. Rev. E., **61** (2000) 2539.
[17] F. Borgonovi, I. Guarneri and F.M. Izrailev, *Phys. Rev. E*, **57** (1998) 5291.
[18] F. Borgonovi, I. Guarneri, F.M. Izrailev and G. Casati, *Phys. Lett. A*, **247** (1998) 140.
[19] V.V. Flambaum, A.A. Gribakina, G.F. Gribakin, and M.G. Kozlov, *Phys. Rev. A*, **50** (1994) 267.
[20] A.A. Gribakina, V.V. Flambaum, and G.F. Gribakin, *Phys. Rev. E*, **52** (1995) 5667.
[21] V.V. Flambaum, A.A. Gribakina, G.F. Gribakin, and I.V. Ponomarev, *Physica D*, **131** (1999) 205.
[22] V.V. Flambaum, in *Parity and Time Reversal Violation in Compound Nuclear States and Related Topics*, Eds.N. Auerbach and J.D. Bowman, World Scientific, 1996, p.41.
[23] N. Rosenzweig and C.E. Porter, *Phys. Rev.* , **120** (1960) 1698.
[24] H.S. Camarda and P.G. Georgopoulos, *Phys. Rev. Lett.*, **50** (1983) 492.
[25] R. Haq, A. Pandey and O. Bohigas, *Phys. Rev. Lett.*, **48** (1982) 1086.
[26] M. Horoi, V. Zelevinsky and B.A. Brown, *Phys. Rev. Lett.*, **74** (1995) 5194; *Phys. Lett. B*, **350** (1995) 141.
[27] N. Frazier, B.A. Brown and V. Zelevinsky, *Phys. Rev. C*, **54** (1996) 1665.
[28] V. Zelevinsky, B.A. Brown, M. Horoi and N. Frazier, *Phys. Rep.*, **276** (1996) 85.
[29] P.Jacquod and D.L.Shepelyansky, *Phys. Rev. Lett.*, **79** (1997) 1837.
[30] B.L. Altshuler, Y. Gefen, A. Kamenev and L.S. Levitov, *Phys. Rev. Lett.*, **78** (1997) 2803.
[31] A.D. Mirlin and Y.V. Fyodorov, *Phys. Rev. B*, **56** (1997) 13393.
[32] B.V. Chirikov, *Phys. Lett. A*, **108** (1985) 68.
[33] D.L. Shepelyansky and O.P. Sushkov, *Europhys. Lett.*, **37** (1997) 121.
[34] D. Weinmann, J.-L. Pichard and Y.Imry, *J. Phys. I France*, **7** (1997) 1559.
[35] V.V.Flambaum and G.F.Gribakin, *Phys. Rev. C*, **50** (1994) 3122.
[36] P.G. Silvestrov, *Phys. Rev. Lett.*, **79** (1997) 3994.
[37] P.G. Silvestrov, *Phys. Rev. E.*, **58** (1998) 5629.
[38] G. Casati, B.V. Chirikov, I Guarneri, and F.M. Izrailev, *Phys. Rev. E*, **48** (1993) R1613.
[39] G. Casati, B.V. Chirikov, I. Guarneri and F.M. Izrailev, *Phys. Lett. A*, **223** (1996) 430.
[40] W. Wang, F.M. Izrailev and G. Casati, *Phys. Rev.*, **E 57** (1998) 323.
[41] Y.V. Fyodorov, O.A. Chubykalo, F.M. Izrailev and G. Casati, *Phys. Rev. Lett.*, **76** (1996) 1603.
[42] A. Bohr and B. Mottelson, *Nuclear structure, Vol. 1* (Benjamin, New York, 1969).
[43] B. Georgeot and D.L. Shepelyansky, *Phys. Lett.*, **79** (1997) 4365.
[44] C. Mejia-Monasterio, J. Richert, T. Rupp and H.A. Weidenmüller, *Phys. Rev. Lett.*, **81** (1998) 5189.
[45] G. Casati, V.V. Flambaum and F.I. Izrailev, to be published.
[46] J.P. Draayer, J.B. French, and S.S.M. Wong, *Ann. Phys. (N.Y.)*, **106** (1977) 472; **106** (1977) 503.
[47] J.B. French, V.K.B. Kota, A. Pandey, and S. Tomsovic, *Ann. Phys. (N.Y.)*, **181** (1988) 235.
[48] B. Lauritzen, P.F. Bortignon, R.A. Broglia, and V. Zelevinsky, *Phys. Rev. Lett.*, **74** (1995) 5190.
[49] V.V. Flambaum, in *Time Reversal Invariance and Parity Violation in Neutron Reactions*, edited by C. R. Gould, J. D. Bowman and Yu. P. Popov (World Scientific, Singapore, 1994), p. 39.
[50] V.V. Flambaum and O.K. Vorov, *Phys. Rev. Lett.*, **70** (1993) 4051.
[51] O.P. Sushkov and V.V. Flambaum, *Usp. Fiz. Nauk*, **136** (1982) 3; [Sov. Phys. Usp., **25** (1982) 1].
[52] V.V. Flambaum, A.A. Gribakina, G.F. Gribakin, and I.V. Ponomarev, *Phys. Rev. E*, **57** (1998) 4933.
[53] I.V. Ponomarev, V.V. Flambaum, A.A. Gribakina, and G.F. Gribakin, cond-mat/9710172.
[54] V.V. Flambaum, A.A. Gribakina, and G.F. Gribakin, *Austr. Journ. Phys.*, **52** (1999) 443.
[55] V.V. Flambaum, G.F. Gribakin and O.P. Sushkov, 1997, unpublished.
[56] F. Borgonovi and F.M. Izrailev, Phys. Rev. E., **62** (2000) 6475.